Hindawi
Geofluids
Volume 2022, Article ID 9962143, 30 pages
https://doi.org/10.1155/2022/9962143

Research Article

A Stepwise Discrimination Method of Multi-Index in Landslide Stability Monitoring

Hao Chen [1,2] and Honggang Wu [2]

[1]*School of Civil Engineering, Lanzhou University of Technology, Gansu 730000, China*
[2]*China Northwest Research Institute Co. Ltd. of CREC, Lanzhou, 730070 Gansu, China*

Correspondence should be addressed to Honggang Wu; 271462550@qq.com

Received 16 June 2022; Revised 17 August 2022; Accepted 2 September 2022; Published 13 October 2022

Academic Editor: Yi Xue

The deep displacement monitoring can directly reflect the deformation information inside the slope and can provide an important evidence for the identification of landslide stability. Based on the monitoring data on deep displacement of borehole, there are many monitoring indicators that can reflect the slope state. However, these indicators have their own applicability, and they are independent of each other, which cannot fully reflect the true movement state of the landslide. Therefore, it is necessary to establish a scientific method to give full play to the strengths of each monitoring index and improve the accuracy of identification for landslide stability. Here, the near-surface accumulative displacement, displacement rate, kinetic energy, and the rate of change of kinetic energy are selected as main monitoring indicators to establish a multi-index stepwise discrimination method for landslide stability in this study. This method analyzes the total deformation characteristics and movement trend of landslide from three aspects: surface displacement, internal displacement rate, and slope energy. Relied on the monitoring data on deep displacement of borehole of a landslide in Wushan County, Chongqing, China, this study finds that a single index is easily disturbed by external factors, causing the abnormal mutation in curve which affects analysis of landslide deformation. The variation characteristics of curve among multiple indexes can be mutually corroborated, effectively identify the abnormal fluctuation of the curve, and avoid the identification errors of landslide movement state. In addition, we also found that when there is an obvious sliding surface on the slope, the displacement rate curve will cluster at the sliding surface along the depth direction in this study. And this feature can be used as an important basis for the identification of sliding surface. The method proposed in this study can provide reference and suggestions for the actual treatment of landslide and monitoring data on deep displacement mining.

1. Introduction

As a common natural disaster, landslide occurs frequently in mountainous areas. With the continuous extension of human economic activities and the extensive construction of various infrastructures in alpine areas, the damage and harm caused by landslide disasters are becoming more and more serious. Timely discovery of hidden dangers, elimination of dangerous situations, and adoption of scientific and effective landslide control measures are the keys to ensuring the safety of people's lives and reducing economic losses, and slope stability monitoring is a prerequisite for these tasks. In the division of landslide deformation stages, Xu Qiang et al. [1] divided it into three stages: initial deformation, constant velocity deformation, and accelerated deformation. And Xu Bangdong [2] further divided the landslide deformation into six developmental stages of creeping, squeezing, fretting, sliding, large-moving, and consolidation based on the characteristics of slope deformation through a large number of landslide research and analysis.

As an important means of slope stability monitoring, landslide deep displacement is generally used to determine the position and trend of slope sliding surface. However, there are still some deficiencies in the degree of data mining and utilization of deep displacement so that many scholars have conducted in-depth research based on deep displacement and summarized the corresponding discriminant indicators and some important conclusions. Ye Xian et al. [3] calculated and analyzed the combined displacement of landslide deep displacement and the main sliding direction. Jin Xiaoguang et al. [4] proposed that the displacement and deformation of the deep part of the landslide have several types of curves, such as V type, D type, B type, r type, pendulum type, and composite type. Each curve shape can reflect the position of sliding surface (or potential sliding surface) and the development process of the landslide deformation and can also reflect the sliding nature of the landslide. Through experimental analysis, Dong Xiujun et al. [5] found that the microscopic displacement-time curve of the slope has a step characteristic and the displacement change can be used as a discriminating index for the deformation stage of the landslide. G.B. Crosta et al. [6] used power law curve fitting for rock mass deformation data, improved the rate-time curve, and defined the rate threshold under emergency management. Chen He et al. [7] segmented the boreholes according to a certain depth from the perspective of energy, calculated the kinetic energy of each segment of soil, and obtained the kinetic energy of boreholes by cumulative calculation. And the slope stability was analyzed by the kinetic energy curve.

When a single index is used to judge the stability of the slope, some indexes are sensitive to the influence of the external environment [8], resulting in a significant change of the curve characteristics, which interferes with the judgment of deformation stage of slope. However, some indicators have strong anti-interference ability and can stably maintain the curve change characteristics, which is beneficial to further identify the deformation stage of the slope [9, 10].

Based on the deep accumulative displacement monitoring data of actual landslide cases, this study analyzes the variation law of different indexes and constructs a multi-index stepwise discrimination method [11, 12]. Through the study, it is found that this method is helpful to identify the deformation stage of slope and can effectively solve the problem of unclear identification of single index. In addition, it is found in this study that the displacement rate curve clusters at different depths of boreholes have more obvious and stable deformation characteristics, which is helpful to determine the position of the sliding surface. The research content of this study provides a new way for slope stability monitoring.

2. Basic Information for the Study Area

2.1. Overview of Landslide. The landslide area is located in Wushan County, Chongqing City, China, and there is a highway passing through the middle. The Daning River is 2.9 km north of it, belonging to the Yangtze River system. The specific location is shown in Figure 1.

The landslide area belongs to the tectonic dissolution and deep valley slope landform area. The surface is a broken line slope between gentle and steep, and the overall slope direction is NNW. The upper part of the slope extends to the Yuba Highway at an elevation of about 520 m, the elevation of the slope top surface is about 430 m, and the lower part extends to the water area of the Daning River. The water level elevation is 172 m, and the valley elevation is about 130 m.

This paragraph needs to be revised.The landslide area is located in the subtropical humid monsoon climate zone, with abundant sunlight and large rainfall. The rainy season is from June to August, and the rainfall is frequent from November to January. The average annual rainfall is 1049.3 mm, and the maximum annual rainfall is 1356 mm. In addition, the maximum monthly rainfall is 445.9 mm, and the maximum daily rainfall is 199.0 mm.

The strata exposed in the landslide area from top to bottom are Quaternary Holocene residual slope (Q_4^{el+dl}), the second member of Middle Triassic Badong Formation (T_2b^2), silty mudstone, and the first member of Middle Triassic Badong Formation (T_2b^1).

The K28+310 ~ K28+900 section of Hurong Expressway passes through the front of the landslide group. The width of the landslide group is about 590 m, and the length is nearly 1000 m perpendicular to the line. The landslide group is an old landslide along the layer of broken rock. According to the landform and the structural characteristics of the slope body, the landslide group is divided into the east landslide and the west landslide. Each landslide can be divided into three blocks: front, middle, and later (Figure 2).

2.2. Monitoring Data Collection. In 2014, the local government carried out a large-scale control of the landslide, and the control project was completed in 2016. In order to strengthen the post-construction monitoring and stability assessment of the landslide, the government entrusted professional institution to carry out long-term continuous monitoring of the slope stability.

The boreholes analyzed in this study are concentrated in the middle-level slide block in the east landslide area. The monitoring data of four boreholes ZK4-1, ZK4-2, ZK4-3, and ZK4-5 at the IV-IV section [13] are selected (Figure 3(a)). The collection time was from October 18, 2017, to January 4, 2019, in which the ZK4-4 drilling instrument was damaged and failed to collect valid data.

3. Data Analysis

3.1. Content Overview. In this study, single-hole analysis was firstly carried out, and the deep displacement of ZK4-1 borehole was selected to calculate its resultant displacement, near-surface accumulative displacement, near-surface displacement rate, kinetic energy, and the rate of change of kinetic energy around the borehole in turn. The data change law of each index is used to determine the position of sliding surface and deformation phase of the slope near the borehole [14]. Then, the development of sliding surface and the overall stability of landslide are comprehensively judged by comparing the variation characteristics of each index in the remaining boreholes.

Figure 1: Landslide position information.

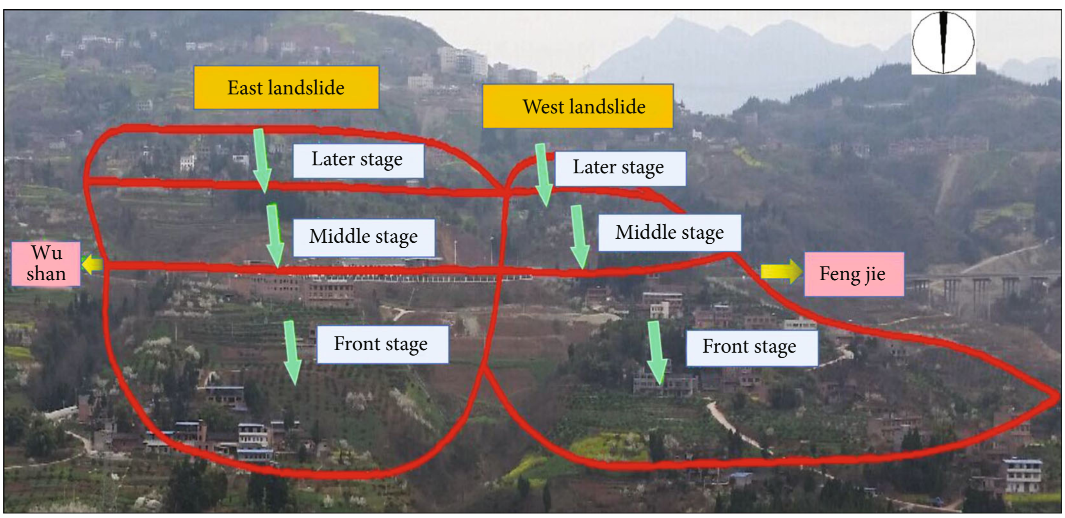

Figure 2: Block diagram of landslide area.

3.2. Single-Hole Analysis

3.2.1. Calculation of Borehole Closure Displacement. The inclinometer is usually used for data collection in the deep displacement monitoring of the slope, which usually includes the displacement data in the A direction and the B direction (perpendicular to the A direction), as shown in Figure 4.

The combined displacement at a certain depth of the inclinometer can be calculated [15, 16] by the following formula:

$$L = \sqrt{X^2 + Y^2}, \quad (1)$$

where L is the resultant displacement at a certain depth of the inclinometer; X is the displacement in direction A; and Y is the displacement in direction B.

Based on the above calculation method, according to the monitoring data on deep displacement of borehole from October 18, 2017, to January 4, 2019, this study analyzes the data variation characteristics of single hole with single day and single hole with multi day and draws the accumulative displacement-depth curve of ZK4-1 borehole in N-S direction and W-E direction and its accumulative resultant displacement-depth curve.

3.2.2. Single Diurnal Displacement of ZK4-1 Borehole. The deep displacement data of ZK4-1 borehole on October 18, 2017, were selected for analysis, and the results are shown in Figure 5.

It can be found from Figure 5 that:

(1) On October 18, 2017, the cumulative displacement-depth curve of ZK4-1 borehole in the NW direction and the EW direction reached 35 mm and 9 mm, respectively, at the depth of 36 m. And it can be

(a) Layout of monitoring points in IV-IV section

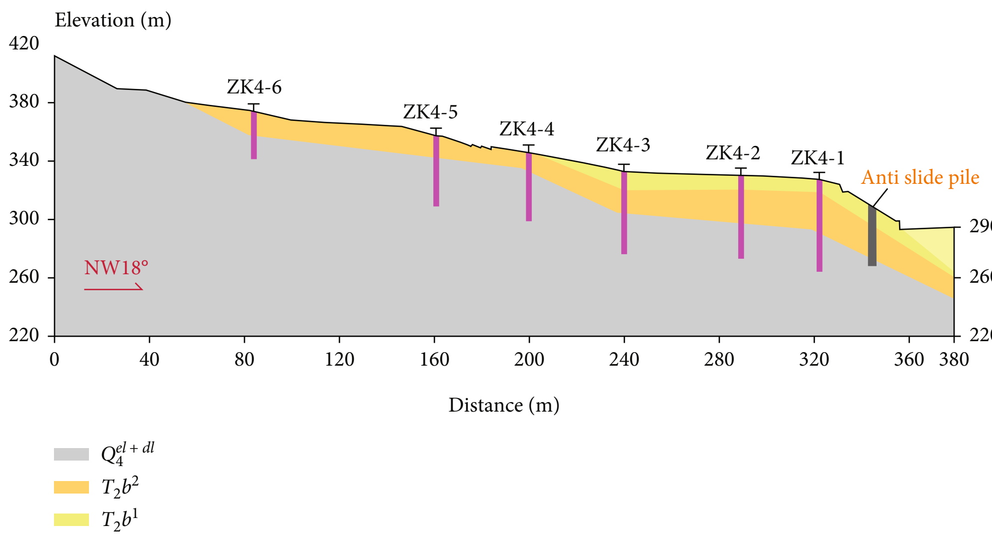

(b) Section IV-IV engineering geological profile

FIGURE 3: Layout of monitoring points and engineering geological profile of section IV-IV (the black section of the IV-IV section in (a) corresponds to the geological structural map shown in (b)).

preliminarily judged that a slip surface has been formed at the depth of 36 m

(2) Figure 5(a) at the depth of 23 m has a significant convex turning point, where the displacement reached10 mm, and Figure 5(b) at the depth does not change significantly, indicating that the depth has a potential slip surface and along the N-S direction development

(3) Within the range of 0 m to 10 m from the surface, the curve in Figure 5(b) changes in a wave-like manner. The two curves in Figure 5(a) and 5(b) both show obvious turning points at a depth of 5 m, and the displacement here is 7 mm which can be inferred that the soil near the surface is relatively soft and a potential sliding surface is formed at the depth of 5 m

(4) By comparing Figures 5(a), 5(b), and 5(c), it can be found that the accumulative displacement-depth curve in the N-W direction has the most significant deformation characteristics and the difference of the mutation points is obvious, which is beneficial to infer the position of sliding surface. The deformation characteristics of accumulative displacement-depth curve in W-E direction are relatively balanced, indicating that the deformation in this direction is small. The deformation characteristics of

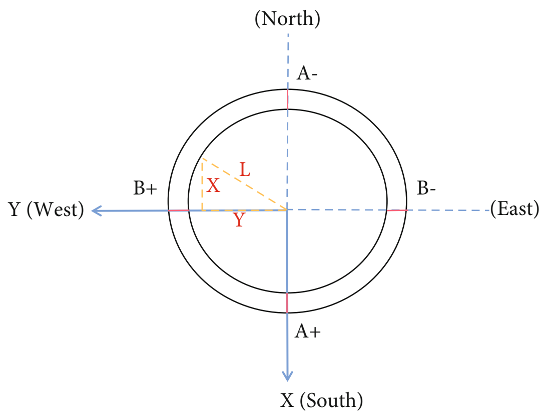

Figure 4: Schematic diagram of combined displacement calculation.

accumulative resultant displacement-depth curve are obvious which have the deformation characteristics of accumulative displacement-depth curve in N-S direction and E-W direction. It can more clearly reflect the deformation of soil at different depths of the borehole and is helpful to judge the overall trend of soil around the borehole

3.2.3. Multi-Day Accumulative Resultant Displacement of ZK4-1 Borehole. For the monitoring data of ZK4-1 borehole from October 18, 2017, to January 4, 2019, the accumulative resultant displacement of the borehole [17] on each day can be calculated by Formula (1). It can be found from Figure 6 that:

(1) At the depth of 50 m, the curve has an obvious turning point, and the displacement reaches 18 mm. Since the maximum depth of the borehole is 50 m, the actual displacement and deformation at this depth cannot be continued, but it can be inferred that there is a potential sliding surface at this depth

(2) Within the range of 36 m-50 m, the curve is "V-shaped" as a whole, indicating that the soil in this section is continuously developing and deforming. The displacement at the depth of 36 m reaches 38 mm, which indicates that the sliding surface has been formed at the depth of 36 m and is in the state of shear creep, and the sliding surface is developing slowly

(3) In the interval range of 5 m-36 m depth, the curves are relatively parallel to each other, and the local fluctuation is obvious which shows a pendulum-shaped distribution. But the swing amplitude is less than 10 mm in the range of measurement error indicating that the soil in the interval is in a relatively stable state

(4) In the range of 0 m to 5 m depth, the accumulative displacement near the surface increased significantly from September 18, 2018, to January 4, 2019, and the accumulative displacement curve at 5 m depth showed a significant turning point. It can be inferred that there was a potential sliding surface at this depth and the sliding surface was not formed at the stage of slow deformation

3.2.4. Near-Surface Cumulative Displacement of ZK4-1 Borehole. The accumulative displacement near surface is the most direct monitor index reflecting the deformation state of slope. The dynamic information of landslide can be quickly obtained according to the change characteristics of the curve [6, 18]. In this study, the displacement data at 0.5 m of ZK4-1 borehole during the monitoring period is selected for analysis. It can be found from Figure 7 that:

(1) During the period from October 18, 2017, to May 8, 2018, the curve grew slowly. After May 8, 2018, the accumulative displacement increased significantly, and the growth rate gradually increased. On September 18, 2018, the curve reached the maximum value, and the accumulative displacement began to gradually decrease and tend to be stable

(2) According to the local meteorological data, several large-scale rainfall weather occurred from May 1, 2018, to October 1, 2018

As the deformation of the slope near borehole shows significant phase variation, it can be roughly divided into three segments: stable phase, ascent phase, and descent phase. Among them, the displacement velocity of increase in the ascent phase is fast and coincides with the local rainfall period, so it can be inferred that the slope is easily affected by rainfall. With the continuous infiltration of rainwater, the self-gravity of the soil increases, and the soil becomes loose gradually which makes the shear strength of the soil significantly reduced. Finally, the soil mass is obviously deformed under gravity. However, there is a certain limit to the permeability of rainwater: The soil near surface is significantly affected by rain, but the soil at the bottom is not obvious. Therefore, the accumulated displacement near the ground surface is greatly affected by the rainwater permeability and soil properties, and cannot fully reflect the overall deformation state of the slope.

3.2.5. Near-Surface Displacement Rate of ZK4-1 Borehole. In order to further analyze the development degree of slope deformation near the borehole, the accumulative displacement-time curve at the depth of 0.5 m near surface was derived to obtain the displacement rate curve at this depth, as shown in Figure 8.

According to the change trend of the curve presented in Figure 8 [19, 20], it can be found that:

(1) The overall change trend of the displacement rate curve at the depth of 0.5 m in borehole is close to a horizontal straight line, which indicates that the curve changes smoothly on the macroscopic level and the slope deformation is in a relatively static state

(2) Amplifying the deformation characteristics of the displacement rate curve, it can be clearly found that

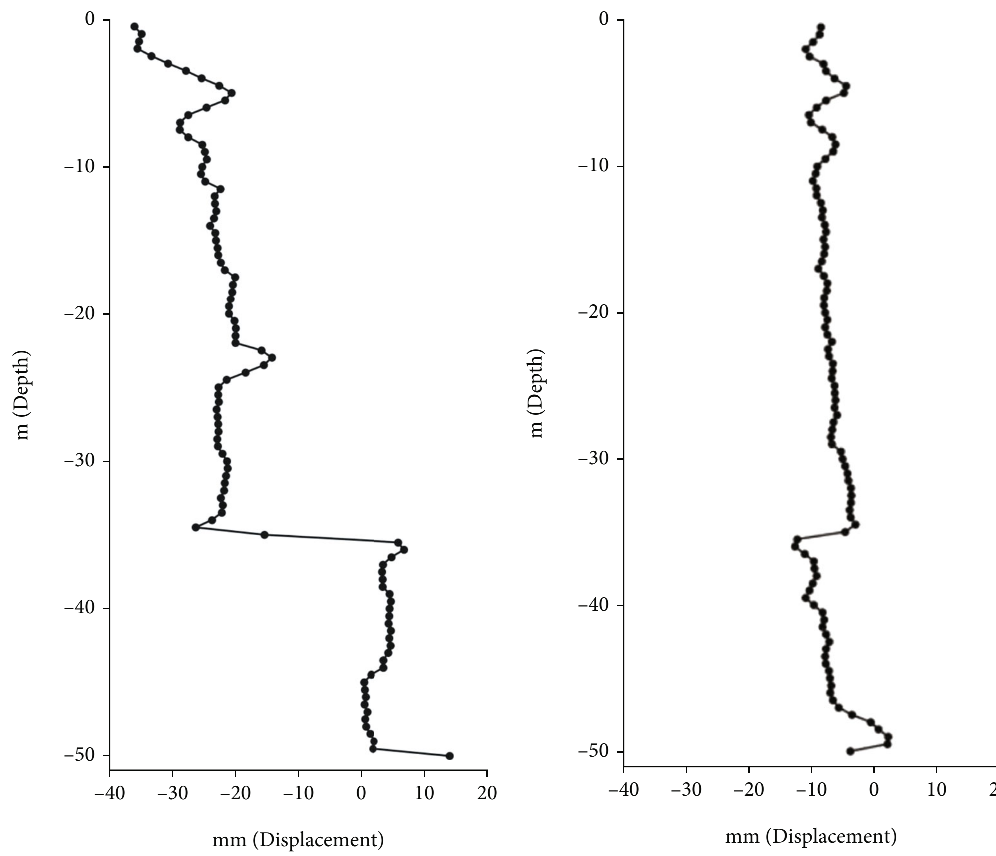

(a) N-S direction

(b) E-W direction

FIGURE 5: Continued.

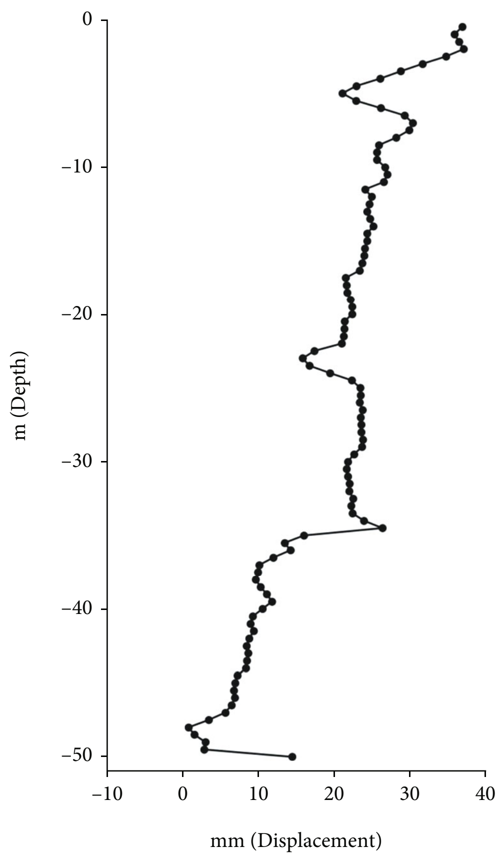

(c) Combined displacement direction

Figure 5: Accumulative displacement-depth curve in N-S and W-E directions and accumulative resultant displacement-depth curve of ZK4-1 borehole (October 18, 2017).

the curve fluctuates around the value of 0 and the maximum value of the rate is only 0.35 mm/day. So it can be judged that the soil deformation around ZK4-1 borehole is weak and the soil deformation rate is very slow

(3) Comparing Figure 7 with Figure 8, it can be found that Figure 7 is biased to identify the growth trend of slope displacement and Figure 8 is in favor of identifying the movement state of slope. Since the basic data of indexes are derived from the displacement change near surface, on the one hand, when the landslide occurs, the soil deformation near surface is the most significant, which helps to quickly extract the important information of slope movement. On the other hand, the slope deformation near surface is significantly affected by environmental factors (such as engineering disturbances and rainfall), which is easy to cause large surface deformation but the overall deformation of slope is weak [21]

Therefore, it is not accurate to judge the deformation of the slope only from the change trend of a certain index related to the near surface. It still needs to be further analyzed and confirmed by other indicators, especially the use of deep displacement data information.

3.2.6. Kinetic Energy and Kinetic Energy Change Rate of ZK4-1 Borehole. The displacement velocity of soil around the monitoring hole is selected to calculate the kinetic energy, as shown in Figure 9. The monitoring hole is divided into several sections according to the sensor layout interval from top to bottom. The kinetic energy of the monitoring hole can be calculated by the following formula:

$$E = \sum_{i=1}^{n} \frac{1}{2} m_i v_{ci}^2 + \frac{1}{2} J_c \left(\frac{|v_{1i}| - |v_{2i}|}{l_i} \right)^2, \quad (2)$$

where m_i is the mass of the cylinder in segment i; v_{1i} and v_{2i} are the upper and lower end velocities of the cylinder in segment i, respectively; v_{ci} is the centroid velocity of the cylinder in segment i; and l_i is the length of the cylinder in segment i; the moment of inertia of the cylinder in segment i of J_c can be calculated by the following formula:

$$J_c = \frac{1}{12} m_i \left(3R^2 + l_i^2 \right), \quad (3)$$

where R is the diameter of the soil around the borehole and r is the diameter of the inclinometer pipe.

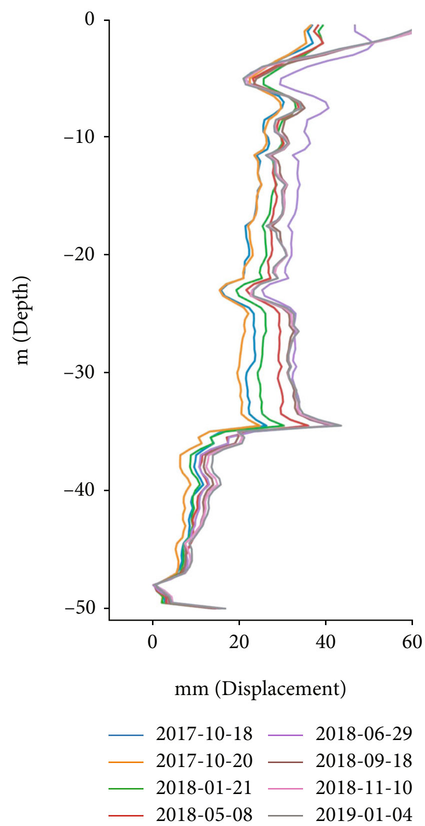

FIGURE 6: Multi-day cumulative displacement-depth curve of ZK4-1 borehole.

Calculate Formula (4) of drilling kinetic energy change rate:

$$\partial E = \frac{dE}{dt}. \tag{4}$$

The kinetic energy and kinetic energy change rate of ZK4-1 borehole can be calculated by Formulas (2), (3), and (4). The calculation results are shown in Figures 10 and 11.

It can be found from Figure 10 that:

(1) The overall change trend of soil kinetic energy around ZK4-1 borehole is close to 0 value horizontal line, indicating that the soil movement near the borehole is weak and in a relatively stable state

(2) Amplifying the change characteristics of the kinetic energy curve, the kinetic energy change during the monitoring period can be divided into two stages: the descending stage and the stable stage. The descending section shows that the slope near the borehole has a moving deformation and is in a state of slow consolidation. The stable section shows that the strength of slope gradually recovers after drainage consolidation and extrusion between the soil and the deformation of the slope gradually weakens or even stagnates

(3) By comparing Figures 7, 8, and 10, it can be found that during the period from May 8, 2018, to September 18, 2019, affected by rainfall, the cumulative displacement curve near the surface of the borehole (Figure 7) showed a significant rise, and the displacement rate near surface of the borehole (Figure 8) also showed significant fluctuations. The kinetic energy change curve of the borehole was close to the horizontal line of 0 value, and there was no obvious fluctuation. By the analysis of near-surface index, the slope appeared obvious movement and deformation in this period. However, the analysis of borehole kinetic energy shows that the slope is not significantly affected by rainfall and the slope movement is weak and is in a stable state as a whole [22]

There are great differences between different indexes for the same slope at the same time, which further proves that judging the deformation of the slope body only from the change trend of a certain index is not necessarily accurate and reliable.

The calculation of slope kinetic energy is to divide the soil in the borehole into several parts. Then, the kinetic energy of soil in each part is calculated based on Formula (3) and finally accumulates the total kinetic energy of the slope near borehole. The monitoring index of kinetic energy gives enough consideration to the combined effect of slope mass and slope velocity within the borehole depth and amplifies the contribution of displacement velocity through the multiple relationship. It improves the anti-interference ability of the indicators, effectively overcomes the shortcoming that the near-surface monitoring indicators are easily affected by the external environment, and can truly reflect the overall movement state of the slope. Therefore, the difference in the calculation methods of each index has a great divergence in the discrimination of the same slope at the same period. It is further proved that it is not always accurate and reliable to judge the deformation of slope only from the change trend of a certain index.

In addition, the kinetic energy index can reflect the state of the whole landslide motion, and considering the kinetic energy change rate of the slope (Figure 11) will help to grasp the movement change trend of the slope.

Therefore, in order to make full use of the deep borehole data, the change rate of kinetic energy (Figure 11) is introduced to analyze the slope deformation.

It can be found from Figure 11 that:

(1) The overall change trend of the soil kinetic energy change rate curve around ZK4-1 borehole is close to the horizontal line of 0 value, indicating that the soil near the borehole has no obvious movement trend and is in a relatively stable state

(2) Enlarging the change characteristics of the kinetic energy change rate curve, the kinetic energy change rate curve during the monitoring period can be divided into three stages: the descending section, the stable section, and the ascending section. The descending segment indicates that the trend of slope movement is gradually weakening. After entering the

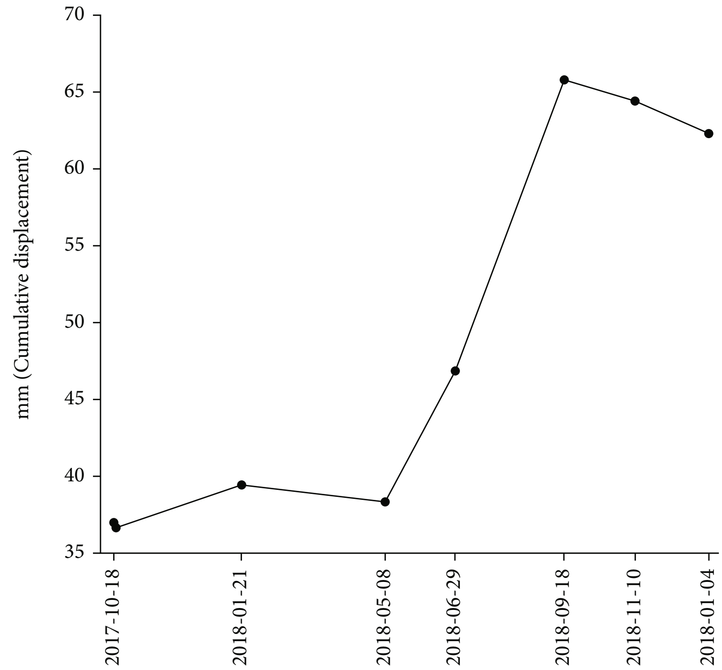

Figure 7: Cumulative displacement-time curve at 0.5 m of borehole ZK4-1.

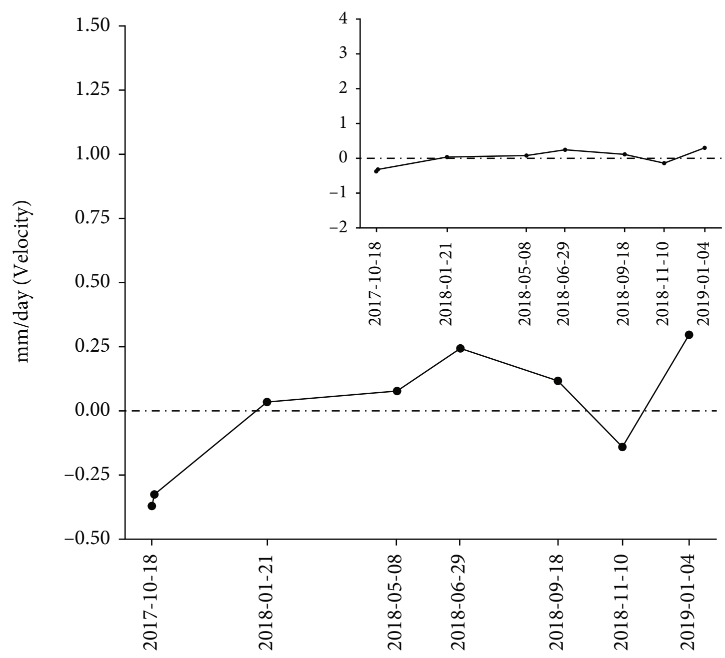

Figure 8: Displacement rate at the depth of 0.5 m in ZK4-1 borehole.

stable stage, the slope is in a relatively static state, and the movement trend is weak. The ascending segment indicates that the trend of the slope movement is gradually highlighted, and there is a potential sliding trend

(3) Since November 10, 2018, the kinetic energy change rate curve has entered the rising stage. Compared with Figure 10, the borehole kinetic energy did not increase significantly during this period, while in contrast with Figure 7, the near-surface displacement rate increased significantly during this period, showing a certain synchronization

As the primary variable that changes with time, velocity is the key parameter that affects the change rate of kinetic energy. Because of the high synchronization between the kinetic energy change rate and the soil displacement rate,

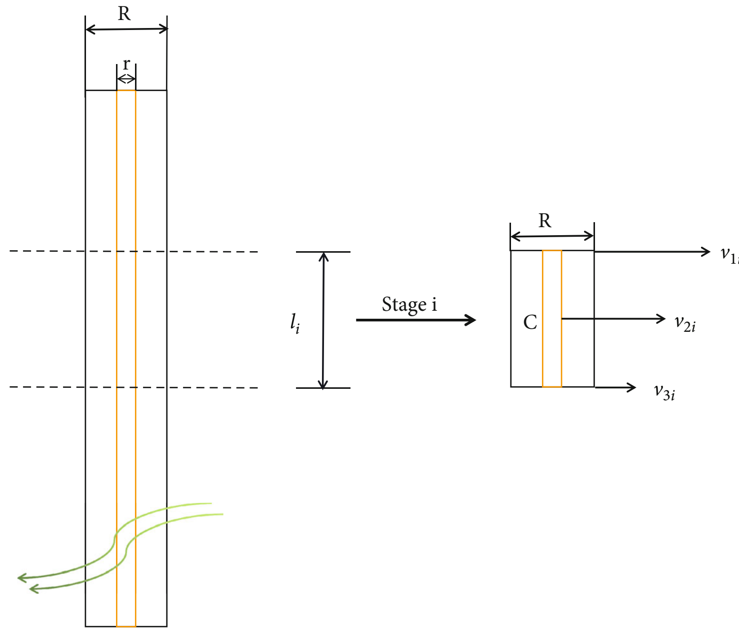

Figure 9: Schematic diagram of borehole kinetic energy calculation.

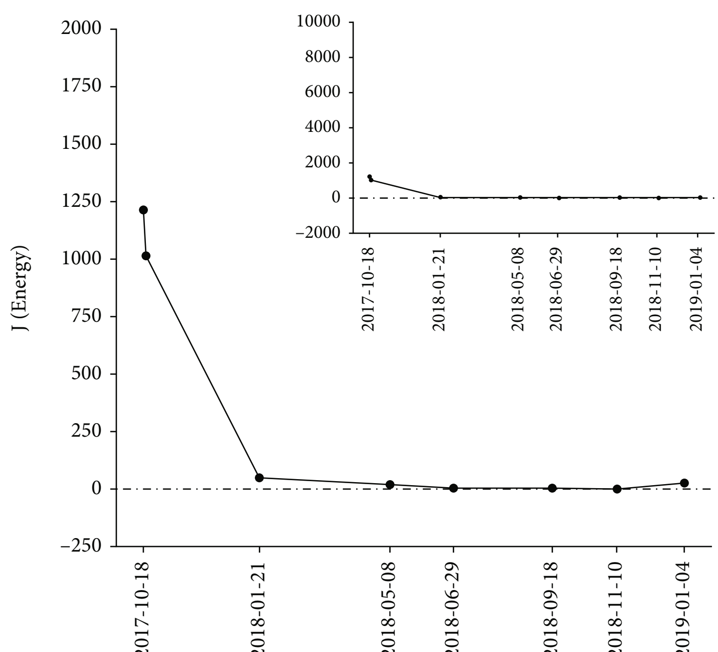

Figure 10: The kinetic energy of ZK4-1 borehole.

the change of soil velocity at different positions within the drilling depth can be significantly amplified. Thus, this index can better reflect the overall trend of landslide movement.

3.3. Joint Analysis of Multiple Boreholes

3.3.1. Analysis of Cumulative Displacement-Depth Curve of each Borehole. The drilling depth of ZK4-1 is 50 m, that of ZK4-2 is 39 m, that of ZK4-3 is 34 m, and that of ZK4-5 is 21 m. The cumulative displacement-depth curves of each borehole are shown in Figures 12 and 13 [23, 24].

From Figures 12 and 13, it can be found that:

(1) The curve variation characteristics of each borehole are obviously different, showing different changes. The accumulative displacement-depth curve of ZK4-1 borehole is relatively close as a whole. The curve is complex and changeable, and the section division is not obvious, but the position of the main sliding surface is easy to determine, which is located at the depth of 36 m. In addition, at the depth of 5 m, the curve bulges obviously, and the displacement

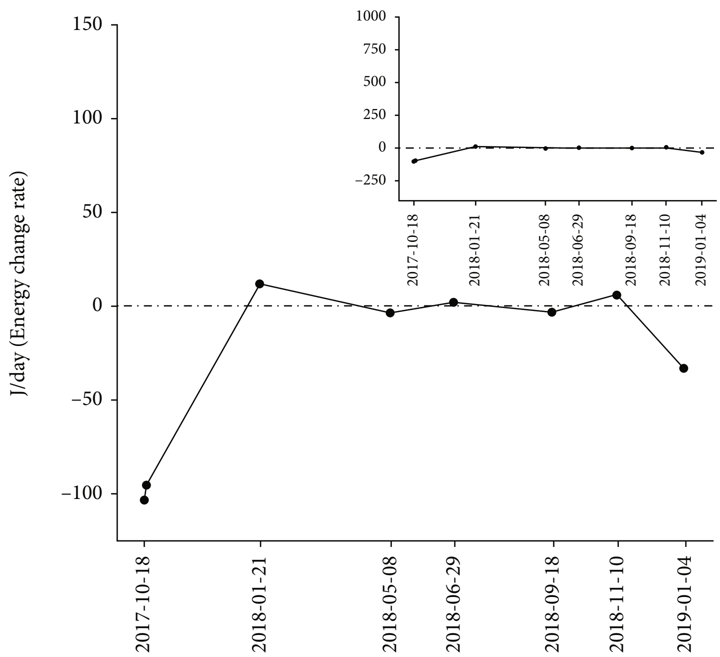

Figure 11: Change rate of kinetic energy in borehole ZK4-1.

reaches 22 mm indicating that there is a potential sliding surface at this depth

(2) The ZK4-2 borehole cumulative displacement-depth curve is overall regular and orderly, and the section interface is obvious. In the depth range from 32 m to 39 m, the interval between the curves is small, and the deformation is weak, indicating that the soil in this section is stable. From 7 m to 32 m in depth, the interval between the curves gradually increases, and the soil in the section shows a trend of overall displacement. And at the depth of 32 m, the accumulative displacement curve shows a sharp increase, indicating that the slip surface at the depth of 36 m has formed and moved slowly. In the depth range from 0 m to 7 m, the interval between the curves increases significantly, and the overall shape is bulging and protruding, indicating that the soil movement in this area is active, and there is formed sliding surface at depth of 5 m

(3) The ZK4-3 borehole accumulative displacement-depth curve segment is clearly divided, and the whole is D-shaped indicating that the sliding surface has been formed. In the depth range from 22.5 m to 34 m, the curve shows a pendulum shape swinging slightly on both sides of the initial value, and the swing amplitude is less than 10 mm which indicates that the soil in this section is in a relatively stable state. In the interval of depth 5 m to 22.5 m, the curves are approximately parallel to each other, showing the characteristics of rigid body motion, indicating that the soil in this section is stable. And the curve has an obvious sudden change at the depth of 22.5 m, indicating that the sliding surface has been formed at this depth. In the interval from 0 m to 5 m in depth, the curve changes stably in the initial period, and the curve shows significant bending changes in the later period, indicating that the slope may have a potential sliding surface at this depth

(4) The overall variation of ZK4-5 borehole accumulative displacement-depth curve is small, and the section division is more obvious. In the section from 5 m to 21 m in depth, the curve interval is small and distributed in a straight line, and the deformation is weak which indicates that the soil in this section is in a stable state. In the section from 0 m to 5 m in depth, the interval between the curves increases and approximates parallel distribution, showing a trend of overall migration. The curve has an obvious sudden increase at the depth of 5 m, indicating that the slope has a potential sliding surface at this depth. In addition, compared with the accumulative displacement-depth curves of other dates, the curve on October 20, 2017, deviates significantly from other curves [25]. Through analysis, it can be found that the accumulative displacement-depth curves after that day did not continue this trend of change, but it is basically consistent with the curve deformation characteristics on October 18, 2017. So it may be caused by the obvious movement of the slope near surface on that day, which made the borehole inclinometer appear spatial deformation with the movement of soil during this period, resulting in the significant increase of the curve in the same day. With the movement and compression of the surrounding soil, the spatial position of the

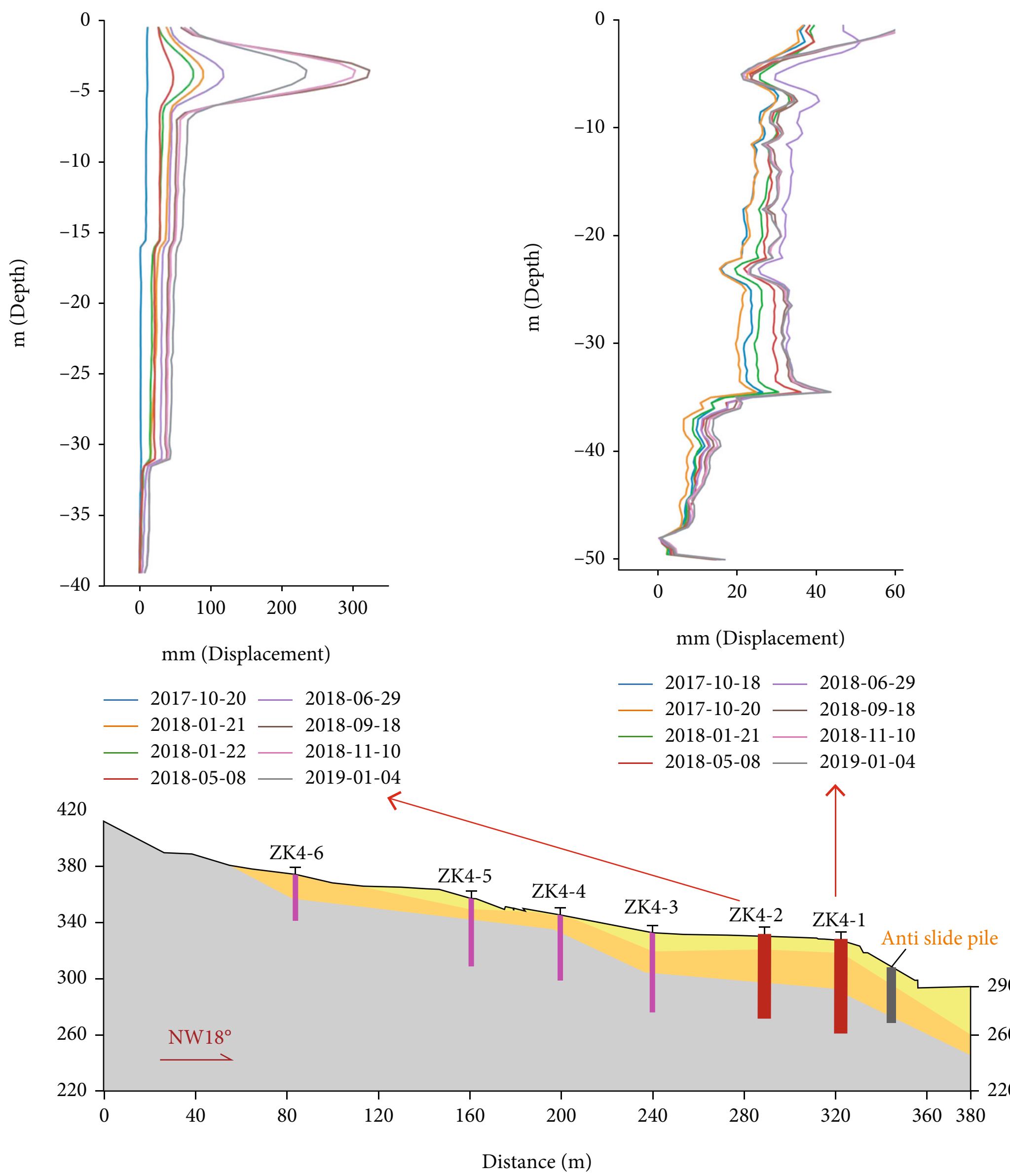

Figure 12: Cumulative displacement-depth curves of ZK4-1 and ZK4-2 boreholes.

inclinometer pipe gradually recovers, making the horizontal displacement of the soil increase in the opposite direction [26].

According to the above analysis results and field exploration report, the slide surface position diagram is drawn. From Figure 14, it can be found that there are two slide blocks on the slope, and the volume of slide block I is small, and the depth of slide surface is shallow. There are two sliding surfaces in the larger volume of block II, which are blocked by the anti-slide pile. The sliding surface at the deeper depth of block II is obviously divided into sections. The traction section is connected with block I, the sliding direction of the main sliding section is similar to that of block I, and the anti-slide section intersects with the anti-slide pile [27, 28].

3.3.2. Cumulative Displacement of Each Borehole Near Surface. It can be found from Figure 15 that the accumulative displacement-time curves of each borehole at the depth of 0.5 m near the surface are significantly different.

(1) Figure 15(a) has the characteristics of typical accumulative displacement increasing with time and has obvious sudden increase section, which can clearly judge the deformation trend of the slope

(2) The curve in Figure 15(b) shows an overall upward trend. Since the data collection interval between January 21, 2018, and January 22, 2018, is only one day apart, and the near-surface accumulative displacement of these two days differs by 13 mm, the data has the characteristics of a sudden drop. During the

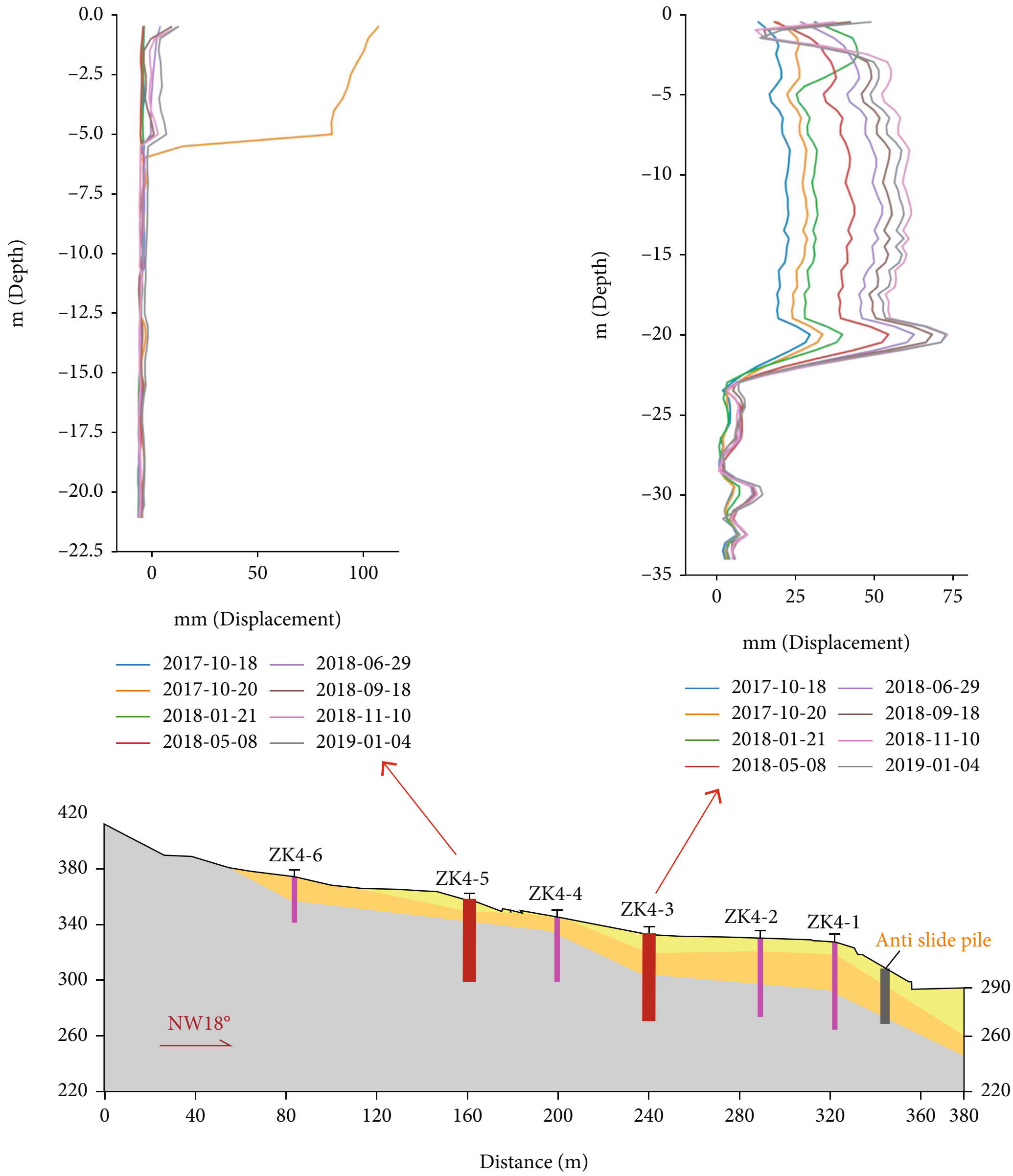

Figure 13: Cumulative displacement-depth curves of ZK4-3 and ZK4-5 boreholes.

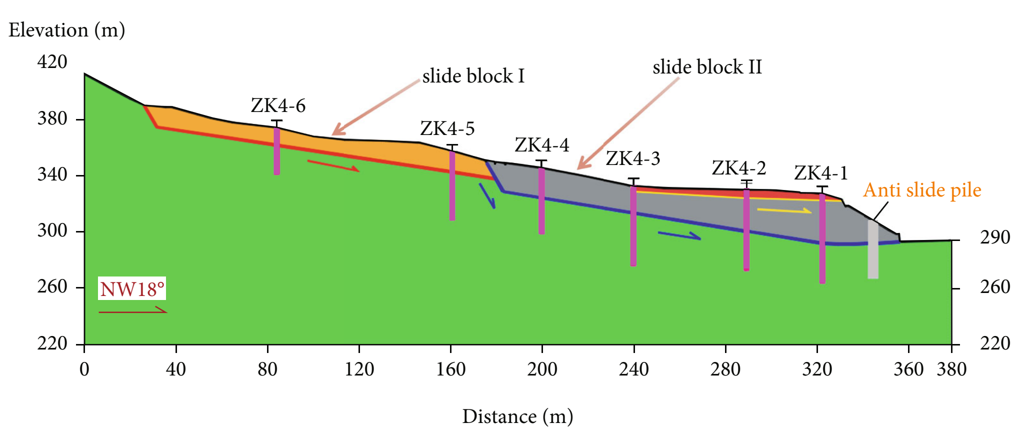

Figure 14: Schematic diagram of sliding surface position.

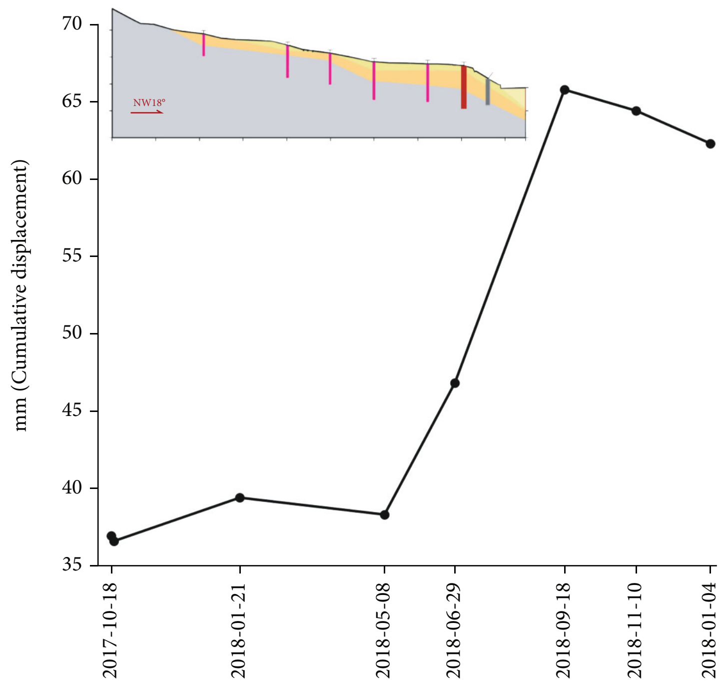

(a) ZK4-1

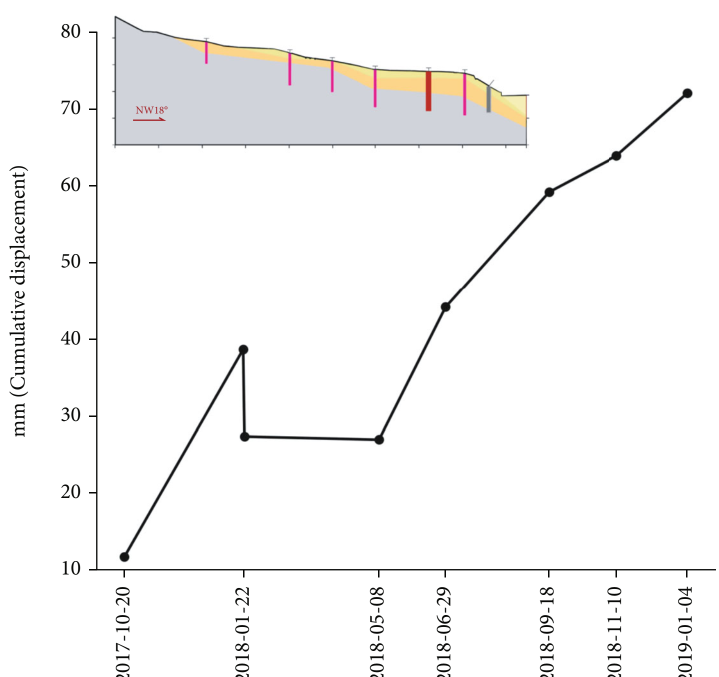

(b) ZK4-2

Figure 15: Continued.

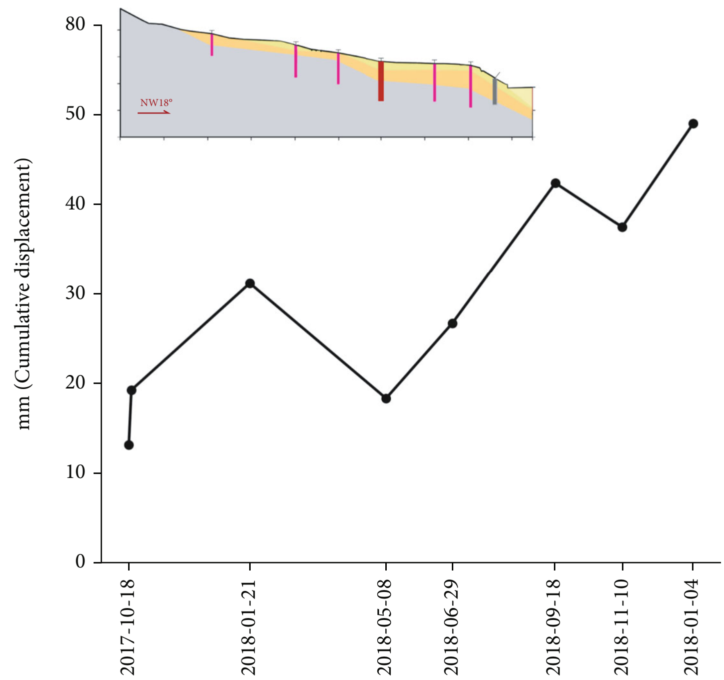

(c) ZK4-3

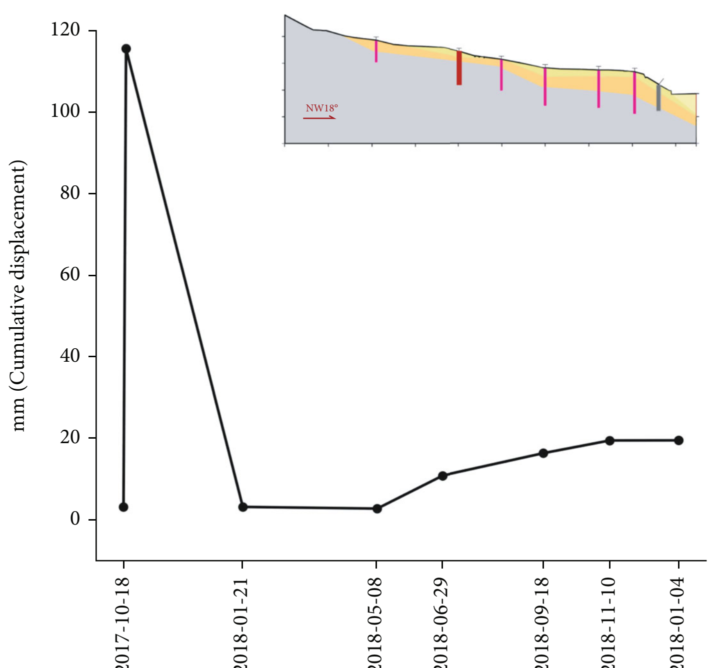

(d) ZK4-5

Figure 15: Cumulative displacement-time curves at 0.5 m depth of ZK4-1, ZK4-2, ZK4-3, and ZK4-5 boreholes.

period from 22 January 2018 to 8 May 2018, the accumulative displacement growth nearly stagnated, while the curve began to rise significantly after 8 May 2018, indicating that the slope near ZK4-2 borehole may be in a slow deformation stage

In Figure 15(c), the accumulative displacement curve rises and falls intermittently, showing a slow fluctuating upward trend as a whole, indicating that the direction of movement of the slope is relatively variable. Due to the small increase in accumulative displacement, the slope is in a relatively stable state.

(3) The curve in Figure 15(d) can be divided into ascent phase, descent phase, and stable phase. By comparing the accumulative resultant displacement-depth curve of ZK4-5 borehole (Figures 13 and 15(d)), it can be found that the accumulative resultant displacement-depth curve increased significantly on

October 20, 2017, and the displacement value of the curve decreased obviously after that day, resulting in apparent rising and falling phase of the curve in Figure 15(d). From January 21, 2018, to May 8, 2018, the curve trend was stable. After May 8, 2018, the curve began to show an uptrend, but the increasing amplitude was small. So it can be inferred that the soil around the borehole is relatively stable as a whole

Therefore, it can be seen from Figure 15 that the curve characteristics at different positions are significantly varied and the displacement information reflected by them is discrepant. In addition, the time interval of data acquisition and the state of slope movement are important factors that affect the deformation characteristics of near-surface accumulative displacement-depth curve. Due to the variability of landslide movement, the curve characteristics of a single borehole cannot clearly grasp the deformation state of slope. The conjoint analysis of multiple boreholes can better obtain the deformation messages in near surface, but the index of accumulative displacement can only reflect the surface information. The stability discrimination for stability of landslide still needs more in-depth analysis.

3.3.3. Near-Surface Displacement Rate of each Borehole. The displacement rate of each borehole near the surface can be obtained by derivation of the accumulative displacement-time curve of each borehole at the depth of 0.5 m. It can be found from Figure 16 that there are obvious differences and similarities in the characteristics of the displacement rate curve of each borehole.

(1) It can be found from Figure 16(a) that the displacement rate near the surface of ZK4-1 borehole fluctuates around 0 and the maximum fluctuation value is 0.3 mm/day, indicating that the slope is in a stable state. Compared with Figure 15(a), the displacement rate curve can better show the actual motion state of the slope

(2) From Figure 16(b), it can be found that the initial value of the displacement rate near the surface of ZK4-2 borehole is large and then gradually decreases. With the passage of time, the rate value gradually approaches 0, indicating that the slope near the surface has obvious activity in the early stage of monitoring and is relatively static in the late stage. Comparing Figure 15(b), it can be found that when the characteristics of accumulative displacement-time curve are complex and it is difficult to judge the slope state, the slope motion state can be more clearly shown by drawing the rate-time curve, which is helpful to identify the slope motion state

(3) From Figure 16(c), it can be found that the characteristics of the displacement rate curve of ZK4-3 borehole are similar to those of ZK4-1 borehole. The curve fluctuates up and down around the zero-value horizontal line, and the maximum value does not exceed 1 mm/day, indicating that the slope movement near the surface is weak

(4) It can be found from Figure 16(d) that the displacement rate curve of ZK4-5 borehole can be roughly divided into three stages: the descending stage, the stationary stage, and the ascending stage. It can be inferred that the deformation rate of the slope near the surface at the initial stage was large and gradually decreased to 0 over time. The slope movement entered a relatively static stage, and the deformation rate of the slope near surface at the later stage began to increase significantly which indicating that there were obvious signs of activity near the surface of the slope. Compared with Figure 15(d), it can be found that there is a quite difference between the two conclusions about the stability state. Figure 15(d) is easy to draw the conclusion that the slope tends to be stable, and in Figure 16(d), curve characteristics show that the slope activity growth trend is obvious

Hence it can be found from Figure [23] that the near-surface displacement rate is significantly dissimilar at different positions of the landslide and the curve deformation characteristics are diverse from each other. Conjoint analysis of near-surface displacement rates at various locations can not only obtain effective information on the deformation speed of slope, but also further identify the accuracy of analysis results of near-surface accumulative displacement curve, which can provide more reliable information for landslide stability analysis [29].

3.3.4. Kinetic Energy of each Borehole. The kinetic energy of ZK4-1, ZK4-2, ZK4-3, and ZK4-5 boreholes can be calculated by Formulas (2) and (3). It can be found from Figure 17 that:

(1) The kinetic energy curve of each borehole approximates a horizontal straight line approaching zero in the overall change trend, indicating that the energy stored in the soil on the cross-section is small and the slope is in a stable state

(2) Enlarging the kinetic energy curve characteristics of each borehole, it can be found that the kinetic energy curves of the three boreholes ZK4-1, ZK4-2, and ZK4-3 have similar variation characteristics and the curves are all L shaped as a whole. In the early stage of monitoring, due to the large displacement rate and the gradual decline, the kinetic energy curve also gradually decreased from the initial large value to a stable stage and finally approached the horizontal line of 0 value, indicating that the kinetic energy accumulated by the slope near ZK4-1 borehole, ZK4-2 borehole, and ZK4-3 borehole gradually dissipated to zero. So the slope movement was weak in a relatively static state

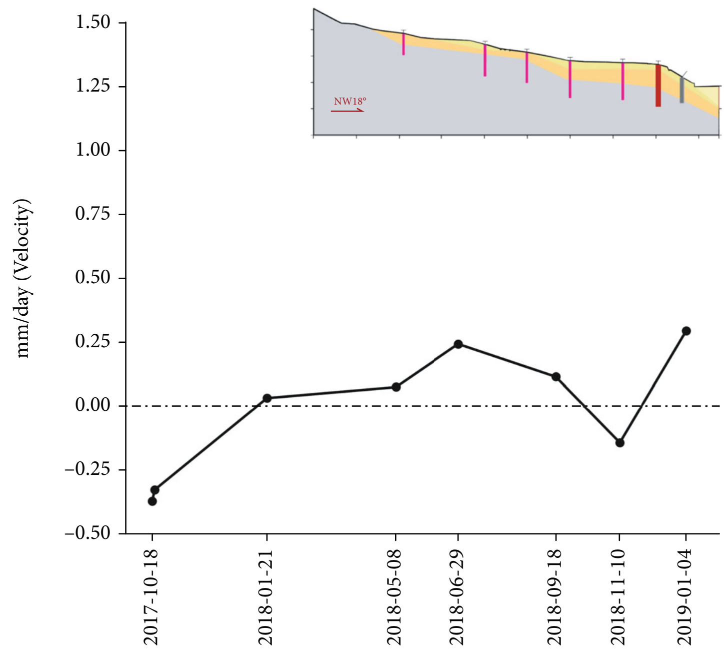

(a) ZK4-1

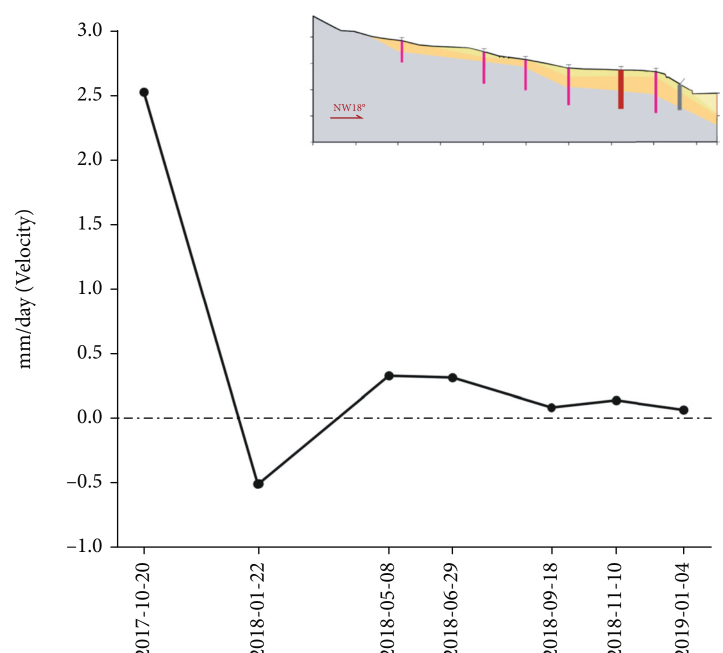

(b) ZK4-2

Figure 16: Continued.

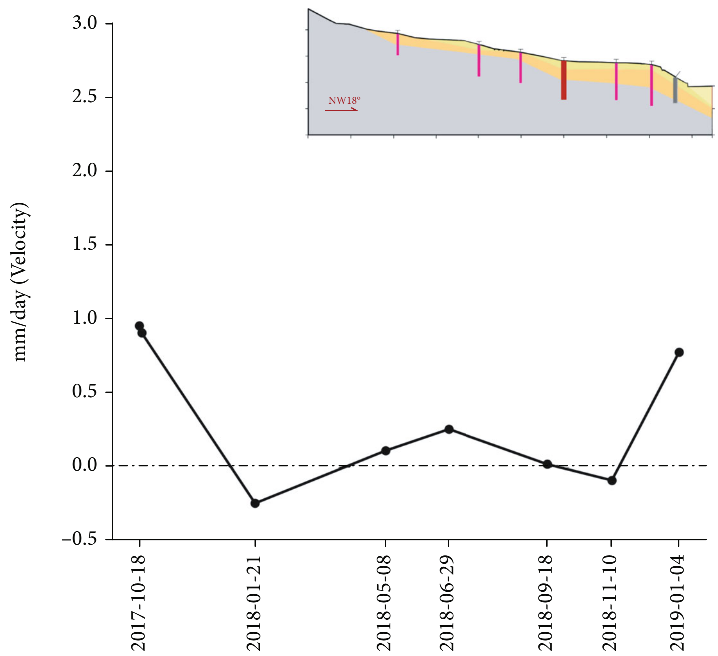

(c) ZK4-3

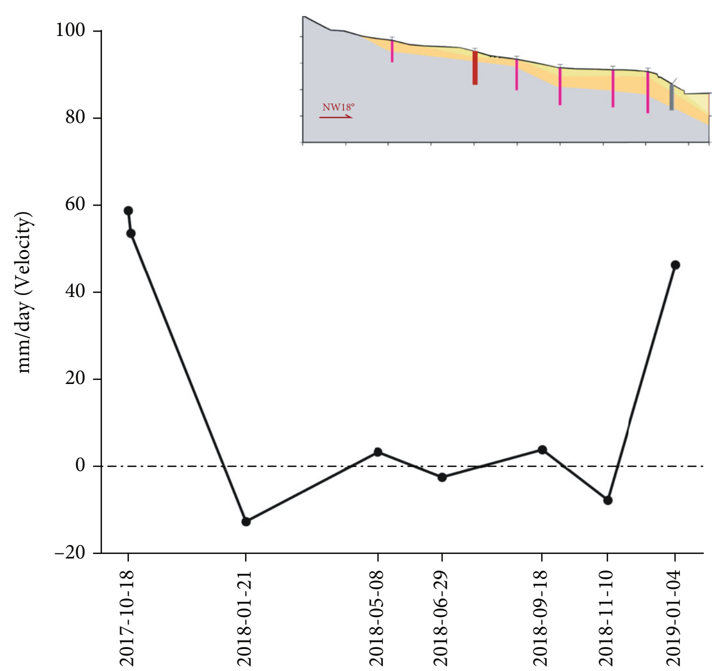

(d) ZK4-5

Figure 16: Displacement rate at 0.5 m depth of ZK4-1, ZK4-2, ZK4-3, and ZK4-5 boreholes.

(3) It can be found from Figure 17(d) that the kinetic energy curve of ZK4-5 borehole is U-shaped, which can be clearly divided into descending section, stable section, and ascending section. In the early stage of monitoring, the kinetic energy of slope decreased gradually, and the soil movement slowed down to a stable stage. The kinetic energy of slope is nearly 0 in the stationary section, and the slope motion is stagnant. At the end of monitoring, the kinetic energy of slope increased significantly, and the slope movement gradually appeared

From the above analysis, it can be found that the distribution of gravitational potential energy on the slope is similar to the characteristics of large top and small bottom due to the inclination on small top and big bottom in the landslide. Therefore, the closer to the slope toe, the smaller is the kinetic energy, and the curve change

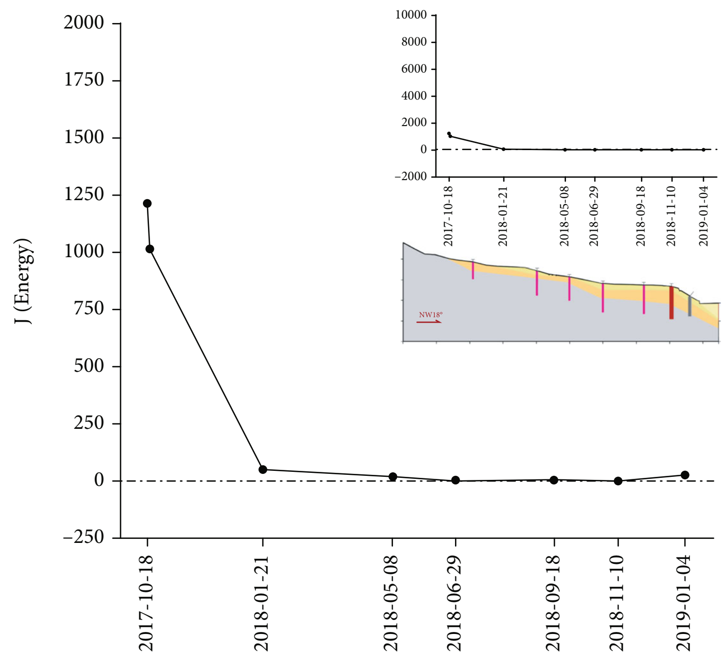

(a) ZK4-1

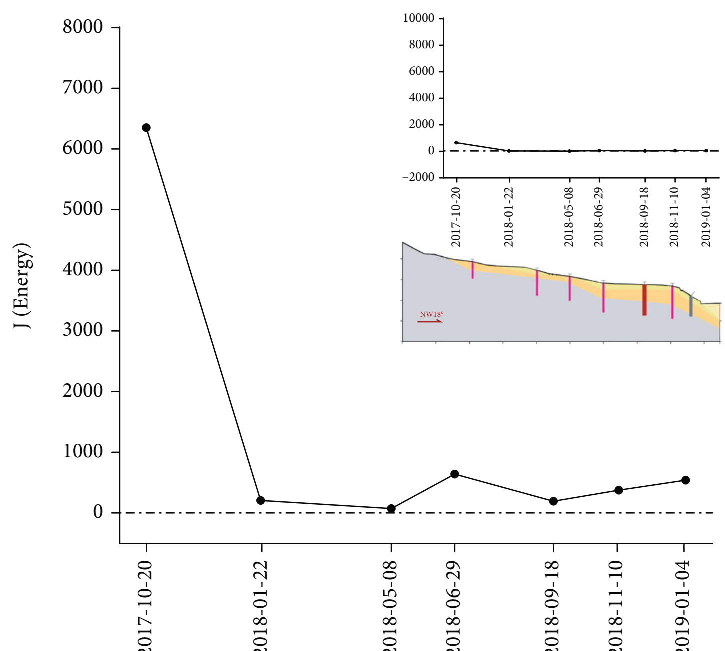

(b) ZK4-2

FIGURE 17: Continued.

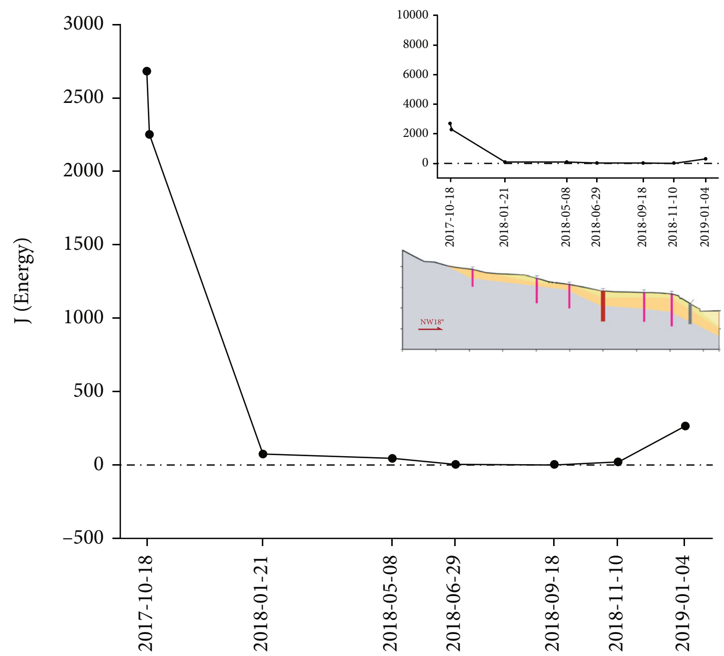

(c) ZK4-3

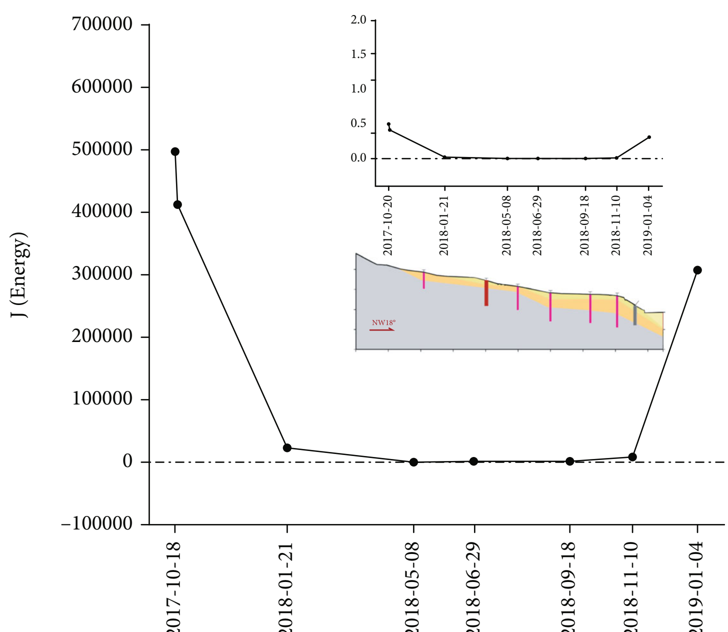

(d) ZK4-5

Figure 17: Kinetic energy of ZK4-1, ZK4-2, ZK4-3, and ZK4-5 boreholes.

characteristics are more flat. According to changes of the kinetic energy at different sites, the overall slope motion state can be comprehensively analyzed which can provide a basis for determining the critical position of the landslide.

3.3.5. Kinetic Energy Change Rate of each Borehole. The kinetic energy of each borehole is derived from Formula (4) to obtain the kinetic energy change rate of the borehole. It can be found from Figure 18 that:

(1) The kinetic energy change rate curve of each borehole approximates a horizontal line approaching zero in the overall trend, indicating that the soil on the section has no obvious movement trend and the slope is in a relatively static state

(2) Enlarging the characteristics of the kinetic energy change rate curve of each borehole, it can be found that the four curves are approximately in the inverted L shape. The trend of the slope movement

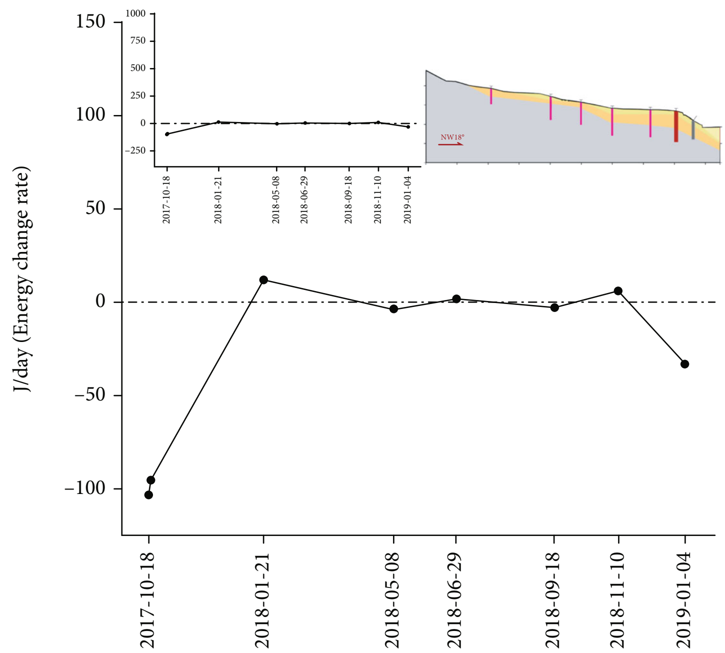

(a) ZK4-1

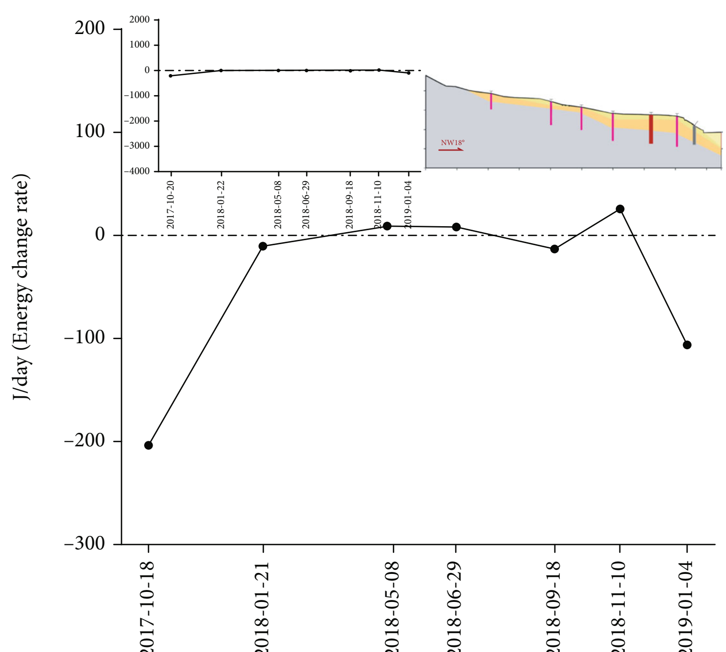

(b) ZK4-2

Figure 18: Continued.

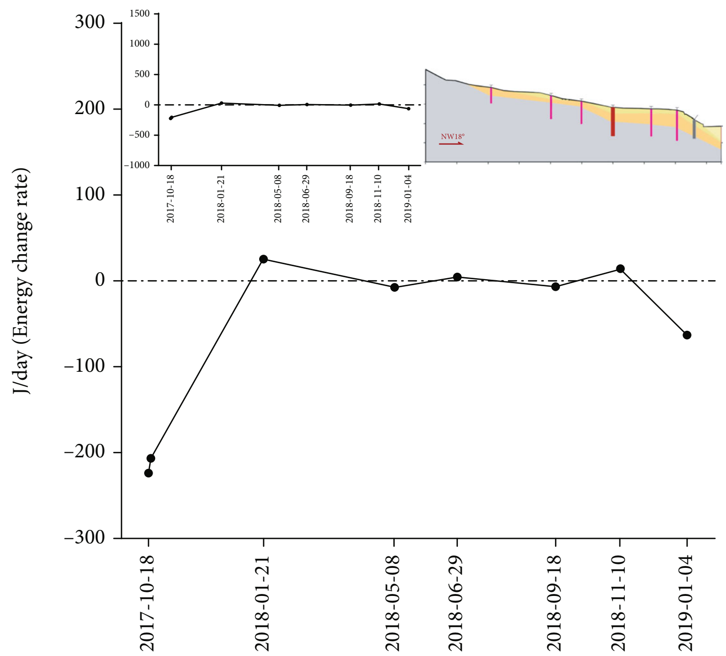

(c) ZK4-3

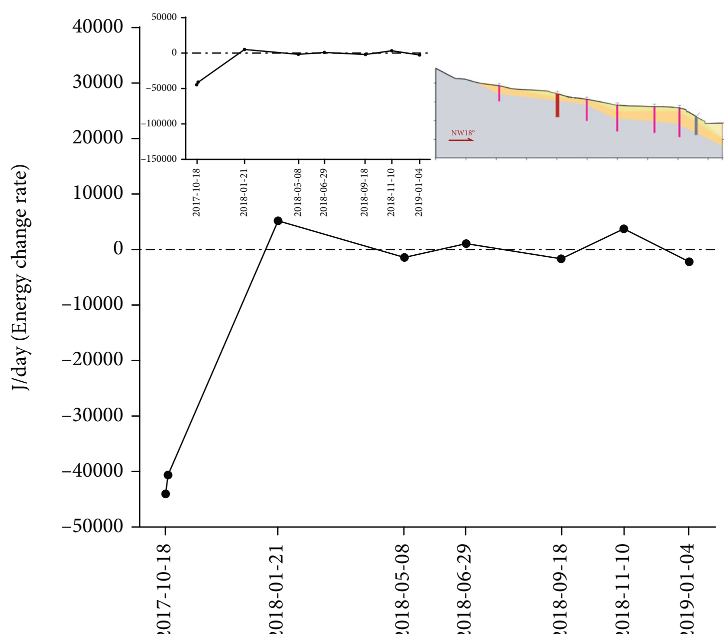

(d) ZK4-5

Figure 18: Change rate of kinetic energy in ZK4-1, ZK4-2, ZK4-3, and ZK4-5 boreholes.

is divided into a descending section and a stable section. Since the curve always oscillates around the 0-value horizontal line after entering the stable section, it shows that the slope movement trend is very weak

(3) Comparing Figures 18(a), 18(b), and 18(c) with Figures 17(a), 17(b), and 17(c), it can be found that the kinetic energy change rate curves show an obvious increase at the tail end, while the kinetic energy curve does not show an obvious increase at the end. In addition, compared with Figures 18(d) and 17(d), it can be found that the kinetic energy change rate curve changes smoothly in the tail section and the kinetic energy curve increases significantly at the tail end. It indicates that the change trend of kinetic energy and kinetic energy of soil near the borehole shows a certain negative correlation in the late monitoring period. When kinetic energy is in steady change, the slope movement trend is gradually increasing. When the kinetic energy increases, the movement trend of slope is gradually declining

By analyzing the kinetic energy change rate curves of each borehole, it can be found that there may exist a negative correlation between the change rate of kinetic energy at different locations and kinetic energy. This characteristic indicates that when the accumulated energy of the slope rises significantly, it does not mean that the slope will have obvious sliding. On the contrary, the slope is still in a relatively static stage at this moment. Combined with kinetic energy and change rate of kinetic energy, the overall movement information and movement trend of landslide can be determined more deeply.

4. Discussion

4.1. Contrastive Analysis. Dong Xiujun [5] obtained the displacement-time curve clusters of landslide deformation and failure under different loading conditions through the physic simulation test with variable angle. The results show that the micro deformation of the sliding zone and the destruction-adjustment of the microstructure of the soil in sliding zone make the displacement-time curve have obvious step features and the size of inclination angle is a sensitive factor affecting the loading condition and the stress state of landslide. Li Cong [30] used statistical method to study the lasted characterized of different deformation stages of landslide. It analyzes the change characteristics of displacement rate of landslide in different deformation stages and considers that the landslide type, failure mode, and sliding surface type are the main factors affecting the deformation rate. Chen He [31] found that the kinetic energy and kinetic energy change rate of landslide have a higher response to the variety of deformation phase by analyzing the variation characteristics and laws of the two indicators at different stages.

These monitoring indexes can better reflect the deformation state and deformation phase of the slope. However, due to the various calculation methods of indicators and monitoring objects, different indicators have certain limitations and have their own applicability:

(1) The characteristics of accumulative displacement curve near surface can reflect the change of soil displacement at the surface

(2) The characteristics of near-surface displacement rate-time curve can reflect the movement state of slope close to the ground and identify the deformation stage

(3) The kinetic energy curve features can estimate the overall movement state of slope from the viewpoints of energy and further identify the deformation stage of slope

(4) According to the characteristics of curve of kinetic energy change rate, the overall movement variation of the slope can be identified, and the motion development state of the landslide can be further mastered

Although each monitoring index can reflect the partial deformation information of the slope, a single monitoring index cannot fully reflect the overall state of landslide. Moreover, the influence factors of each index are not the same, and the curve variation characteristics of each other are obviously different. Therefore, it is easy to misjudge the slope stability by using a single index.

By analyzing the calculation methods of various monitoring indicators, we found the methods of indicators have obvious correlation order:

(1) The data of near-surface accumulative displacement originates from the statistic of accumulative resultant displacement-time curve close to the ground

(2) The rate of near-surface displacement is derived from the time derivative of near-surface accumulative displacement

(3) The borehole kinetic energy is based on the displacement rate of soil at different depths and is obtained by using Formula (3) and accumulating the calculation results

(4) The change rate of borehole kinetic energy is acquired by deriving the borehole kinetic energy from time

Therefore, forming a calculation method of multi indexes by connecting different indicators in series according to the calculation order can not only improve the utilization of the monitoring data on deep displacement of borehole, but also comprehensively reflect the overall deformation state of slope and further improve the reliability and accuracy of stability discrimination. Based on the actual case, the study makes a deep analysis on the slope stability by using the multi-index stepwise discrimination method. The results show that the single index can easily cause abnormal changes under the influence of rainfall, human activities, and other factors and interfere with the identification of slope deformation stage. Multiple monitoring indicators can judge the deformation state of landslide step by step, which can give full play to the advantages of each indicator, and corroborate the reliability of information from each indicator and significantly improve the accuracy of landslide stability identification.

4.2. Analysis and Suggestion of Method Improvement. Based on the monitoring data on deep displacement of single borehole, this study analyzes the movement and deformation information of soil within the drilling depth from the perspective of displacement, velocity, and energy. However, the analysis and exploration of the interaction between the boreholes are not sufficient, and more systematic research is needed. Because the landslide movement is a real-time transform process, the monitoring indicators have different response at various locations of landslide, and the single borehole can only reflect the soil state at that location during the monitoring period. If we can add several typical landslide cases and systematically analyze the interaction between different monitoring indicators at different

Table 1: Applicability of each index.

Index	Advantage	Defect
Cumulative combined displacement	(1) The curve changes obviously and can quickly identify the position of sliding surface (2) The variety of curves helps to distinguish the degree of soil softness at different depths	(1) Affected by the deformation of the inclinometer itself, the data is prone to abnormal distortion, resulting in abnormal curve fluctuations
Cumulative displacement near surface	(1) It can clearly show the growth of slope displacement near the surface	(1) It is easy to be affected by sampling time interval and slope movement state, and it is difficult to grasp the slope deformation state with complex curve changes (2) Displacement variation of deep soil cannot be reflected
Displacement rate near surface	(1) It can clearly reflect the change of slope displacement rate near the surface and obtain the movement information of soil near the surface (2) It is not easy to be affected by sampling interval and slope motion state (3) It can corroborate or correct the judgment result of the cumulative displacement near the surface for the motion state of the slope	(1) It cannot reflect the displacement change of deep soil (2) It is sensitive to abnormal data reflection, which can easily lead to curve mutation, resulting in misjudgment of results
Kinetic energy	(1) It can reflect the kinetic energy of soil in the borehole depth and obtain the motion state of the whole slope (2) It is not easily affected by abnormal data	(1) It is easily affected by the depth of the borehole, and the kinetic energy varies greatly between different boreholes (2) When analyzing kinetic energy curve, it is necessary to manually adjust the coordinate scale to obtain the overall trend of kinetic energy
Rate of change of kinetic energy	(1) It can reflect the change of soil kinetic energy in borehole depth and obtain the overall movement trend of slope (2) It can support or correct the discriminant results of kinetic energy for slope motion state	(1) It is sensitive to abnormal kinetic energy data and easily leads to curve mutation, resulting in misjudgment (2) When analyzing the curve of kinetic energy change rate, it is necessary to manually adjust the coordinate scale to obtain the overall change trend of kinetic energy change rate

positions, it will help to identify the state of landslide motion more accurately.

In addition, the curve change characteristics of the monitoring indicators are important for identifying the landslide movement state, and the selection of coordinate-scale will also affect the determination of landslide stability. If the observing scale is set too large, the curve characteristics are not significant and the key information cannot be highlighted. If the observing scale is set too small, the information with low correlation with the state of landslide movement will be amplified, and the increase of interference information is not conducive to the identification of landslide phase. Therefore, it is an important content of future research to establish a scientific basis for coordinate-scale selection.

Through the single hole analysis and multi hole conjoint analysis, this study discusses the change characteristics of five curves, including accumulative resultant displacement-depth curve, near-surface accumulative displacement-time curve, displacement rate-time curve near the surface, kinetic energy-time curve, and kinetic energy change rate-time curve. In order to facilitate the follow-up research and provide reference for future method improvement, this study summarizes the advantages and disadvantages of each indicator (Table 1).

4.3. Characteristic Analysis of Displacement Rate Curve Cluster. During the research, we found that the distribution characteristics of the soil displacement rate curve at different depths can more fully reflect the deformation characteristics of the slope, and there is a certain relationship with the sliding surface.

(1) It can be found from Figures 19(a), 19(b), and 19(c) that the displacement rate curve clusters of ZK4-1, ZK4-2, and ZK4-3 boreholes have obvious similarities. The curve clusters of the three boreholes fluctuate up and down slightly around the 0 value and approximate a horizontal line approaching the 0 value, indicating that the slope movement near the borehole is weak and the slope is in a stable state

(2) It can be found from Figure 19(d) that the variation characteristics of the curve cluster can be obviously divided into the descending section, the stationary section, and the ascending section, indicating that the movement of the slope body is gradually weakening at the early stage of monitoring. After entering the stationary section, the slope body is in a relatively static state, and the movement state of the slope body

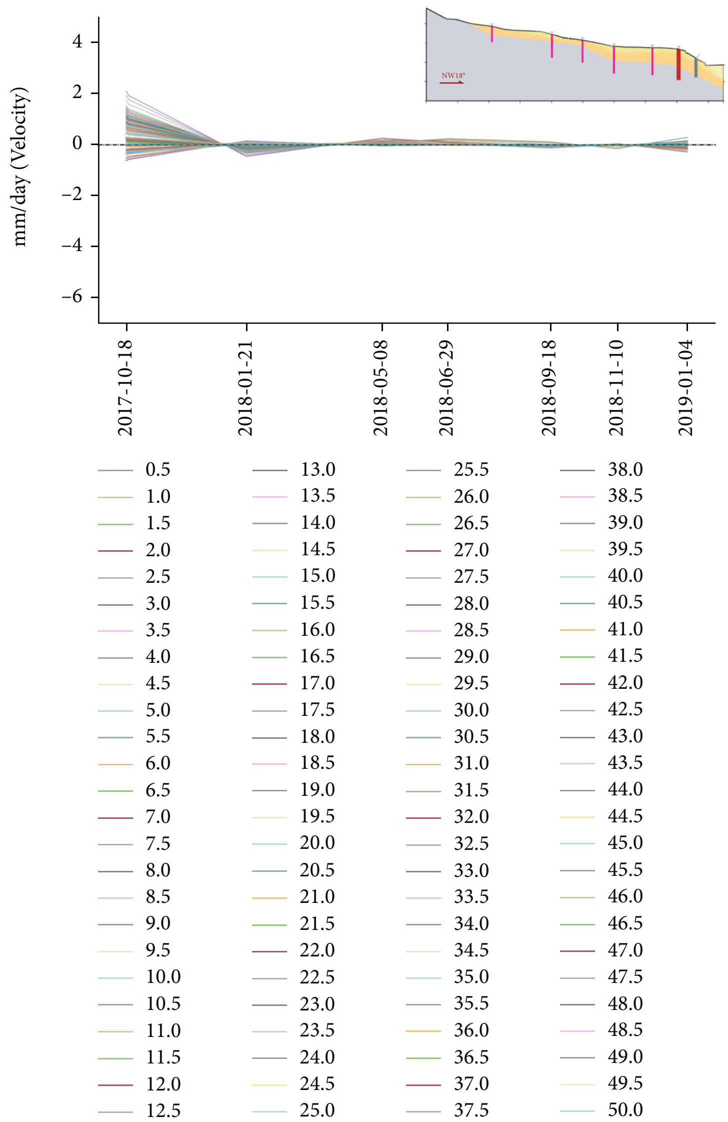

(a) ZK4-1

Figure 19: Continued.

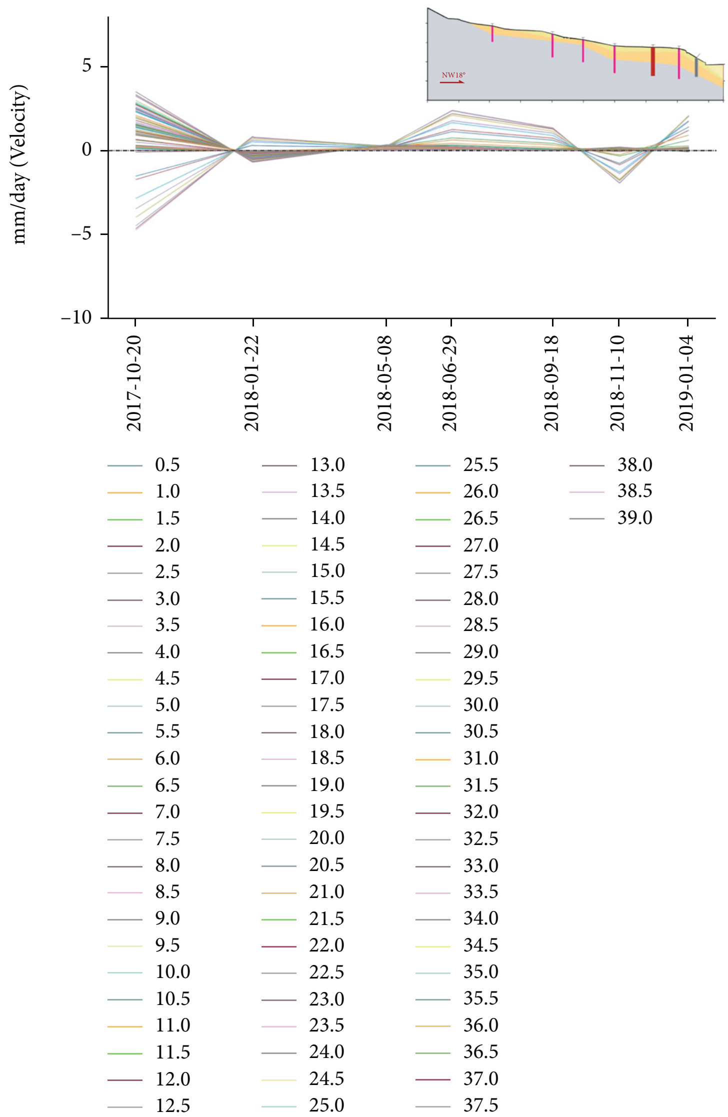

(b) ZK4-2

Figure 19: Continued.

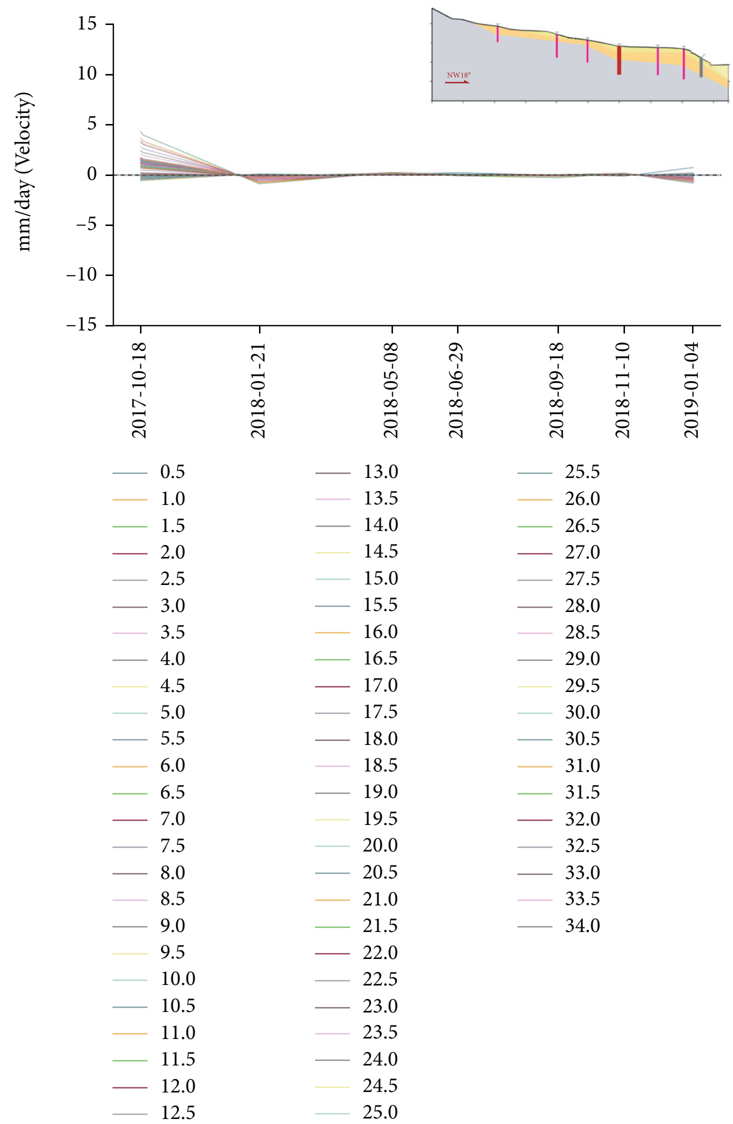

(c) ZK4-3

Figure 19: Continued.

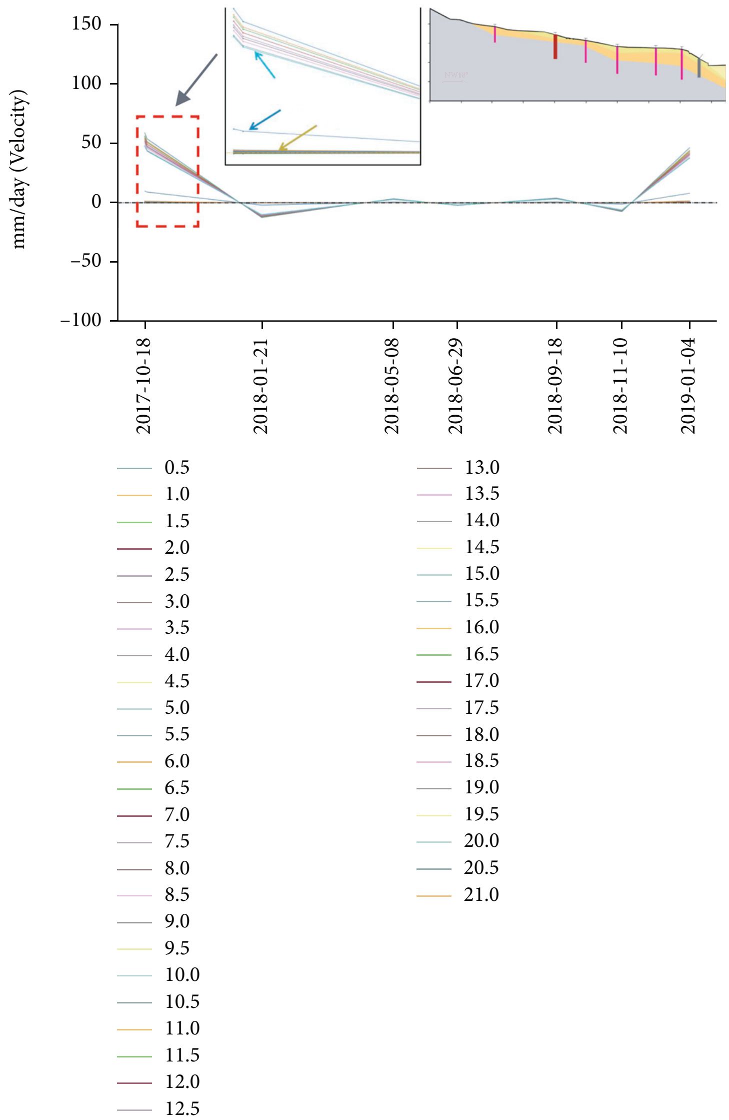

(d) ZK4-5

Figure 19: Displacement rate curve cluster at different depths of ZK4-1, ZK4-2, ZK4-3, and ZK4-5 boreholes (ZK4-1 borehole is 50 m deep with an interval of 0.5 m; ZK4-2 borehole is 39 m deep with an interval of 0.5 m; ZK4-3 borehole is 34 m deep with an interval of 0.5 m; and ZK4-5 borehole is 21 m deep with an interval of 0.5 m).

is gradually becoming active and weak moving at the late stage of monitoring

(3) From Figure 19(d), it can be found that since there is only one rate curve at 5.5 m, the curve clusters can be generally divided into 0-5.0 m and 6.0-21 m groups, and the rate curve at 5.0 m depth is the dividing line of the two groups of curves. By comparing the accumulative displacement-depth curves of ZK4-5 borehole in Figure 13, it is found that the sliding surface is located at the depth of 5.0 m and the position of the sliding surface corresponds to the boundary point in Figure 19(d).

From the above analysis, it can be found that the displacement rate curve cluster in the borehole can reflect the overall movement state of slope on the one hand and help to further confirm the position of the sliding surface on the other hand. The displacement rate of soil at different depths is closely related to the upper slider, sliding surface, and lower sliding bed. Future research can start with the deformation characteristics of the three, analyze the root cause of the clustering characteristics of the displacement rate curve, and establish the relationship between the rate curve and the position of the sliding surface.

5. Conclusions

In this study, a large landslide in Wushan County, Chongqing City, China, was taken as the research object. The cumulative displacement-depth curve, near-surface displacement rate-time curve, kinetic energy curve, and kinetic energy change rate curve were analyzed, and the applicability of each index was summarized. The following conclusions and findings are obtained:

(1) Based on the monitoring data on deep displacement of borehole, this study proposes a multi-index stepwise discrimination method for landslide stability, which is composed of near-surface accumulative displacement, near-surface displacement rate, kinetic energy, and change rate of kinetic energy. This method identifies the state and trend of slope motion step by step from the different dimensions of displacement, velocity, and energy. The advantages of different monitoring indicators are complementary, and the problem of inaccurate identification of the deformation state of the slope body with a single indicator is effectively overcome. The advantages of different monitoring indicators complement each other, which effectively overcome the problem of inaccurate identification of slope deformation state with a single index

(2) By drawing the displacement rate curves at different depths within the borehole range that combined with the change characteristics of curve cluster is helpful to obtain the movement state of landslide. When the landslide has obvious sliding surface, the velocity curve will produce obvious clustering characteristics, which can be used as an important basis for identifying the position of sliding surface

(3) The conclusions and findings put forward in this study are helpful for surveyors to identify the phase of landslide more accurately and to make good use of monitoring data on deep displacement of borehole. And it can significantly reduce various cost of human material resources in landslide monitoring, as well as providing an important reference for stability monitoring and treatment of landslide

Data Availability

The data used to support the findings of this study are available from the corresponding author upon request.

Conflicts of Interest

The authors declare no conflict of interest.

Authors' Contributions

Hao Chen and Honggang Wu are co-first authors.

Acknowledgments

The work described in this study was supported by the National Key R&D Program of China (No. 2018YFC1504901), Gansu Province Youth Science and Technology Fund program, China (Grant No. 21JR7RA739), Natural Science Foundation of Gansu Province, China (Grant No. 21JR7RA738), Science and Technology Development Project of China Railway Research Institute Co., Ltd. (2017-KJ008-Z008-XB), and Science and technology development project of China Railway Ninth Bureau Group Co., Ltd. (DLF-ML-JSFW-2021-09). The financial support is gratefully acknowledged. The authors sincerely appreciate the Broadvision Engineering Consultants for the geological survey information and Mr. Weiyang Zhou for his advice on the status of the landslide.

References

[1] Q. Xu, "Deformation and failure behavior and internal mechanism of landslide," *Journal of Engineering Geology*, vol. 2, no. 20, pp. 145–151, 2012.

[2] X. Bangdong, *Landslide analysis and prevention*, China Railway Press, Beijing, 2008.

[3] X. Ye, Y. Gao, and G. Li, *Calculation and Analysis of Hole Closure Displacement of Landslide Deep Displacement Monitoring*, vol. 10, Highway, 2020.

[4] X. G. Jin, X. H. Li, L. S. Wang, and X. Q. Wang, "Deep displacement curve characteristics and stability identification of landslide," *Journal of Mountain Science*, vol. 18, no. 5, pp. 440–444, 2000.

[5] X. Dong, Q. Xu, C. Tang, and F. Yang, "Characteristics of landslide displacement-time curve by physical simulation experiment," *Journal of Engineering Geology*, vol. 23, no. 3, pp. 401–407, 2015.

[6] G. B. Crosta and F. Agliardi, "How to obtain alert velocity thresholds for large rockslides," *Physics and Chemistry of the Earth, Parts A/B/C*, vol. 27, no. 36, pp. 1557–1565, 2002.

[7] H. Chen, Y. J. Li, R. Fang, and G. Li, "A novel technique for monitoring deep displacement and early-warning of landslide," *Chinese Journal of Rock Mechanics and Engineering*, vol. 34, no. 2, 2015.

[8] L. L. Liang, J. Yang, and M. K. An, "Application of deep hole monitoring in Kaotang landslide treatment," *Subgrade Engineering*, vol. 5, 2008.

[9] O. Hungr, S. Leroueil, and L. Picarelli, "The Varnes classification of landslide types, an update," *Landslides*, vol. 11, no. 2, pp. 167–194, 2014.

[10] S. D. Li, X. Li, J. Wu, and Y. Liu, "The evolution process and model of sliding zone of large bedrock bedding landslide," *Chinese Journal of Rock Mechanics and Engineering*, vol. 26, no. 12, 2007.

[11] D. Stead and A. Wolter, "A critical review of rock slope failure mechanisms: the importance of structural geology," *Journal of Structural Geology*, vol. 74, pp. 1–23, 2015.

[12] W. Y. Xu, Y. F. Hu, W. W. Wu, C. C. Qin, and L. Wei, "Safety evaluation of multi-source information fusion landslide based on cloud model and D-S evidence theory," *Journal of Hohai University (Natural Sciences)*, vol. 50, no. 1, pp. 59–66, 2022.

[13] X. G. Wu, Y. Xia, and Z. H. Xin, "Application of deep hole displacement monitoring technology in landslide investigation," *Subgrade Engineering*, vol. 5, 2010.

[14] S.-l. Zhang, Z.-h. Zhu, S.-c. Qi, Y.-x. Hu, Q. Du, and J.-w. Zhou, "Deformation process and mechanism analyses for a planar sliding in the Mayanpo massive bedding rock slope

at the Xiangjiaba Hydropower Station," *Landslides*, vol. 15, no. 10, pp. 2061–2073, 2018.

[15] J. H. Cai, J. L. Wang, J. H. Deng, and Y. G. Zhou, "United monitoring and analysis on the stability of high slopes for expressway," *Geotechnical Investigation &Surveying*, vol. 12, 2009.

[16] H. Yu and Y. Y. Zhou, "Principle of deep hole displacement dynamic monitoring and its application in landslide control," *Technology of Highway and Transport*, vol. 3, 2008.

[17] H. Chen, H. Liu, and C. W. Liu, "Application of comprehensive displacement monitoring technology in landslide treatment," *Transportation Science & Technology*, vol. 3, 2021.

[18] G. Herrera, J. A. Fernández-Merodo, J. Mulas, M. Pastor, G. Luzi, and O. Monserrat, "A landslide forecasting model using ground based SAR data: the Portalet case study," *Engineering Geology*, vol. 105, no. 3-4, pp. 220–230, 2009.

[19] Q. Xu, Z. Yp, J. P. Qian, C. J. Wang, and C. J. He, "Study on a improved tangential angle and the corresponding landslide pre-warning criteria," *Geological Bulletin of China*, vol. 28, no. 4, pp. 501–505, 2009.

[20] W. H. Zhang, Y. Liu, and X. P. Peng, "Borehole inclinometer curve in Qinglong landslide, Guizhou Province application of stability identification," *The Chinese Journal of Geological Hazard and Control*, vol. 20, no. 1, 2009.

[21] T. W. J. van Asch, L. P. H. Van Beek, and T. A. Bogaard, "Problems in predicting the mobility of slow-moving landslides," *Engineering Geology*, vol. 91, no. 1, pp. 46–55, 2007.

[22] L.-t. Zhan, X.-g. Guo, Q.-q. Sun, Y.-m. Chen, and Z.-y. Chen, "The 2015 Shenzhen catastrophic landslide in a construction waste dump: analyses of undrained strength and slope stability," *Acta Geotechnica*, vol. 16, no. 4, pp. 1247–1263, 2021.

[23] J. Song, "A multi-block sliding approach to calculate the permanent seismic displacement of slopes," *Engineering Geology*, Q. Fan, T. Feng, Z. Chen, J. Chen, and Y. Gao, Eds., vol. 255, pp. 48–58, 2019.

[24] Q. X. Huang, J. L. Wang, and J. H. Deng, "Slope deformation character analysis based on monitoring results of multiple multi-point borehole extensometer," *Chinese Journal of Rock Mechanics and Engineering*, vol. 28, no. 1, 2009.

[25] C. H. Lin and M. L. Lin, "Evolution of the large landslide induced by typhoon Morakot: a case study in the Butangbunasi River, southern Taiwan using the discrete element method," *Engineering Geology*, vol. 197, pp. 172–187, 2015.

[26] N. D. Rose and O. Hungr, "Forecasting potential rock slope failure in open pit mines using the inverse-velocity method," *International Journal of Rock Mechanics and Mining Sciences*, vol. 44, no. 2, pp. 308–320, 2007.

[27] C. He, X. Hu, D. D. Tannant, F. Tan, Y. Zhang, and H. Zhang, "Response of a landslide to reservoir impoundment in model tests," *Engineering geology*, vol. 247, no. 247, pp. 84–93, 2018.

[28] D. F. Yang, X. L. Hu, C. Xu et al., "Model test on the deformation evolution characteristics of landslide with multiple sliding zones," *Bulletin of Geological Scienceand Technology*, vol. 41, no. 2, pp. 300–308, 2021.

[29] R. Romeo, "Seismically induced landslide displacements: a predictive model," *Engineering Geology*, vol. 58, no. 3-4, pp. 337–351, 2000.

[30] C. Li, J. B. Zhu, B. Wang, Y. Jiang, X. Liu, and P. Zeng, "Critical deformation velocity of landslides in different deformation phases," *Chinese Journal of Rock Mechanics and Engineering*, vol. 35, no. 7, pp. 1407–1414, 2016.

[31] H. Chen, H. Tang, X. R. Ge, and Y. J. Li, "Research on early warning of creep landslide by early-warning indictors based on deep displacements," *Chinese Journal of Rock Mechanics and Engineering*, vol. 38, no. 1, 2019.